

# TITANIUM DIOXIDE PHOTOCATALYSIS: FUNDAMENTALS AND APPLICATION ON PHOTOINACTIVATION

**Pedro Magalhães, Luísa Andrade, Olga C. Nunes and Adélio Mendes**

LEPABE, Departamento de Engenharia Química, Faculdade de Engenharia, Universidade do Porto, rua Dr. Roberto Frias, 4200-465 Porto, Portugal

Received: April 02, 2017

**Abstract.** TiO<sub>2</sub> semiconductor is being investigated and used for different applications such as energy production, photoinactivation, photoabatement, self-cleaning and water desalination. TiO<sub>2</sub> has, however, a large band gap, ca. 3.2 eV, which limits its absorption to UV light range that accounts only for ca. 5% of the solar spectrum energy. Therefore, strategies for reducing its band gap aiming to enhance visible light harvesting and making TiO<sub>2</sub> usable for indoors applications are being studied; this reduction is mainly achieved by doping and decoration. More recently, TiO<sub>2</sub>/graphene composite proved to be an interesting material for photocatalytic purposes, presenting enhanced energy harvesting properties and an improved photocatalytic activity. Furthermore, the micro size of the composite graphene platelets allows its use without the potential health hazards associated to TiO<sub>2</sub> nanoparticles. TiO<sub>2</sub> may contribute to prevent nosocomial infections because, similarly to the phagocytic cells of the human immune system, it uses the cytotoxic effects of Reactive Oxygen Species (ROS) to inactivate microorganisms. These ROS are known to be highly reactive with biological molecules and thus they are effective for the inactivation of various types of microorganisms. The photocatalysis fundamentals and the preparation of more efficient TiO<sub>2</sub> photocatalysts suitable for indoor applications are reviewed aiming their application for the photoinactivation of microorganisms. Additionally, a comparison of the effectiveness of photoinactivation with traditionally used disinfection methods is also made. Finally, gaps in the knowledge on the long-term effect of the utilization of TiO<sub>2</sub> based materials are identified.

## 1. INTRODUCTION

In the past four decades photocatalysis fundamentals and applications developed tremendously. Presently, there is a deeper understanding of the photocatalysis fundamentals and, consequently, the use of photocatalysts in several emergent fields such as energy production (e.g. photocatalytic water splitting [1]), environmental protection (e.g. self-cleaning materials [2] and photo abatement of atmospheric pollutants such as NO<sub>x</sub> [3], volatile and halogenated hydrocarbons [4]), water purification (e.g. photooxidation of micropollutants [5], volatile organohalide compounds, pesticides [6]) and for microorganisms inactivation [7].

Even though the environmental applications are leading the photocatalysis, microorganism photoinactivation is also catching more and more attention within the scientific community. In fact, there is an alarming increase in the number of hospital-acquired infections, also known as nosocomial infections [8]. This increase was caused by an uncontrolled use of substances that promote the propagation of antibiotic resistance, strongly motivated by a lack of adequate legislation [9]. Infectious diseases are becoming again a real threat, with new infections appearing at an alarming rate [10], and the exponential movement of people across coun-

Corresponding author: O.C. Nunes, e-mail [opnunes@fe.up.pt](mailto:opnunes@fe.up.pt) and A. Mendes, e-mail: [mendes@fe.up.pt](mailto:mendes@fe.up.pt).

tries, oceans and continents are intensively contributing to their propagation.

In the past decade many studies reported the photocatalysis use for disinfection purposes; especially the antimicrobial application of titanium dioxide has been widely discussed in many reviews and research papers [11]. In this work, the microorganism photoinactivation main issues will be reviewed, namely regarding the development of materials with enhanced visible light harvesting to foster photocatalysis for indoor applications (e.g. hospitals, health centres, etc.). Since the use of TiO<sub>2</sub> for disinfection purposes is being limited to its ability of absorbing only UV light and by the rapid recombination of separated positive and negative charges, doping, decoration and the use of TiO<sub>2</sub>/graphene composites are addressed below as mechanisms for mitigating these drawbacks.

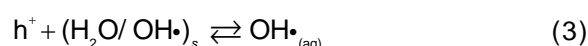
## 2. FUNDAMENTALS OF PHOTOCATALYSIS

The pioneer work developed by Fujishima *et al.* [12] describing water splitting with a TiO<sub>2</sub> photoelectrode caught the attention of several research groups working on this field and rapidly TiO<sub>2</sub> became the most used semiconductor for photocatalysis. Titanium dioxide exhibits three crystalline structures: rutile, anatase and brookite. Rutile is the most thermodynamically stable crystal structure of titanium dioxide but anatase is the preferred form for photocatalysis because it presents higher photocatalytic activity and it is easier to prepare. Brookite is the least stable phase and normally not used in photocatalysis. There are studies that indicate the benefits of mixings different crystalline phases of TiO<sub>2</sub> for obtaining a higher photoactivity [13,14]. When different crystalline phases are coupled, it is mostly believed that the movement of electrons from the rutile phase to the anatase phase occurs, which causes a more efficient e<sup>-</sup>/h<sup>+</sup> separation and consequently an increased photocatalytic activity [15]. However, there are other studies defending that the electron movement is from anatase to rutile [16].

The anatase band gap is ca. 3.2 eV while the band gap of rutile is ca. 3.0 eV. Upon excitation with photons presenting energy higher than the band gap energy, an electron is injected from the valence to the conduction band, generating an electron-hole pair in the conduction and valence bands, respectively – Eq. (1). The photogenerated charges diffuse to the surface of the semiconductor particle where they promote redox reactions; holes may generate vacancies on TiO<sub>2</sub> surface or excited reduced spe-

cies, while excited electrons normally react with oxygen to produce free radical O<sub>2</sub><sup>•-</sup>. These are responsible for the photodecomposition of organic compounds, where adsorbed water and oxygen have been described to play an important role.

There are, nowadays, several proposed pathways for the photodegradation of pollutants [17,18]. The most commonly assumed photodegradation mechanism is based on Langmuir-Hinshelwood kinetic model, as described by Ollis and Turchi [19]:



where OH<sup>•</sup> is the hydroxyl radical, O<sub>2</sub><sup>-</sup> is the superoxide radical and S is an active center of the photocatalyst. This kinetic model was proposed based on studies of spin trapping and electron spin resonance (ESR) showing high concentrations of OH<sup>•</sup> radicals in photocatalytic systems [19]; the presence of hydroxylated intermediates formed during the photodegradation of the studied compounds also supports the suggested model. However, Ângelo [20] reported recently a maximum of NO conversion of 82.4% for a feed containing 25% of RH and of X<sub>NO</sub> = 75.7% for a feed with a dew point of -20 °C; the same work indicates that the water-adsorbed monolayer is reached for a relative humidity of ca. 25%. If the main intermediate oxidation species of NO is OH<sup>•</sup> the NO conversion for the dry feed should be quite smaller, see Eq. (3). This result along with other studies reported in literature [21] question the role of hydroxyl radicals in photocatalysis or, otherwise, of the equation (3). Montoya and co-workers [22] made a strong case against the direct reaction of a photogenerated hole with adsorbed water or OH<sup>-</sup> to form OH<sup>•</sup>, suggesting a novel direct-indirect model (D-I) – Fig. 1. The D-I model shows two different types of interfacial charge transfer mechanisms. For strong electronic interaction, D-I model assumes that photo-oxidation is mainly based in an interfacial direct transfer (DT) mechanism of photogenerated valence band free holes to adsorbed species to TiO<sub>2</sub> surface. On the

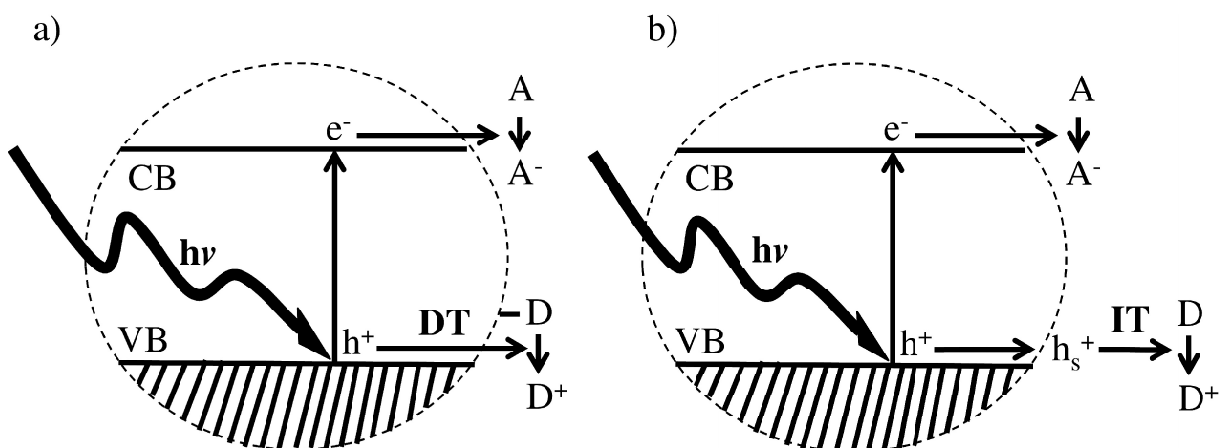


**Fig. 1.** Schematic of the Direct-Indirect Model: a) Direct Transition; b) Indirect Transition. Adapted from [13] with permission.

other hand, for weak interactions between reactant and  $\text{TiO}_2$  surface, the D-I model assumes an interfacial indirect transfer (IT) mechanism involving two successive steps: at the first step,  $h_1^+$  species are trapped by  $\text{O}_s^{2-}$  terminal oxygen ions of the  $\text{TiO}_2$  surface leading to generation of terminal  $\text{O}_s^{\cdot-}$  radicals; at a second step, surface trapped holes are isoenergetically transferred via tunneling to the adsorbed reactant, according to the Marcus-Gerischer model for adiabatic electron transfer at the semiconductor electrolyte interface [23].

The study conducted by Salvador and co-workers [24] analyze the importance of oxygen on the photocatalytic phenomenon. Dillert et al. [25] and Angelo et al. [20], also highlighted the importance of oxygen on the photocatalytic phenomenon, showing that without oxygen there is no NO conversion. Thus, the photooxidation mechanisms still a matter of debate.

As previously mentioned, improving the  $\text{TiO}_2$  photocatalytic activity for attaining visible light activity is being targeted; this improvement can be achieved by: i) avoiding the recombination of photogenerated electrons/holes; ii) narrowing the semiconductor band gap ( $E_g$ ) [26]. While the first permits to efficiently generate more free radicals, the later allows the photocatalyst to absorb a larger fraction of the solar spectrum. Even though the recombination rate of  $e^-/h^+$  has been neglected in many works due to difficulties in its estimation, it has been proved that the recombination rate has a strong contribution for the net photocatalytic activity [27,28]. The majority of the authors working on this topic defend that the crystal structure of the photocatalyst is a dominant factor of the photocatalytic activity since the recombination of  $e^-$  and  $h^+$  is

facilitated at the traps on the surface and in the bulk of the particles [29]. Indeed, it is assumed that the recombination process occurs at the crystal defects, explaining why amorphous  $\text{TiO}_2$  presents almost negligible photocatalytic activity. Nevertheless, there are few works discussing this point since the defects of the photocatalytic powders are very difficult to determine. Anatase absorbs only wavelengths smaller than 386 nm, which falls in the UV range. Sunlight spectrum comprises only 5-7 % of UV light, 46% of visible light and 47% of infrared radiation [30]. So,  $\text{TiO}_2$  modifications to allow visible absorption are fundamental to enhance the photocatalytic rate. Targeting this enhancement the research was directed for the use visible light instead of only UV radiation, and of proper immobilization of the photocatalyst.  $\text{TiO}_2$  doping and/or decoration with the objective of increasing photoactivity and photoabsorbance is addressed below. Doping concerns adding foreign chemical elements (impurities) to modify in the inner-structure of the photocatalyst, while decoration concerns adding materials to the photocatalyst surface. Both modifications target the same objectives: preventing  $e^-/h^+$  recombination and red-shift of the light absorption.  $\text{TiO}_2$ /graphene composite photocatalysts reduces the charge recombination and originates Ti-O-C bonds that promotes significant red-shift.

## 2.1. Doping and decoration

Doping of  $\text{TiO}_2$  can help the improvement of photocatalytic activity by enhancing the optical absorption of wide band gap semiconductors, increasing the minority carrier diffusion length or enhancing the catalytic activity at the surface of the semiconduc-

tor [31]. However, in some cases, these dopants can also promote  $e^-/h^+$  recombination with the creation of mid gap surface states that actually act as recombination centres [31]. High values of dopant concentration (not above  $10^6 \text{ mol}\cdot\text{dm}^{-3}$  [31]) should be avoided since may lead to segregation of the dopant phase. There are two possible doping sites in  $\text{TiO}_2$ : at the titanium site (cation doping) or at the oxygen site (anion doping). Thus, there are two main types of  $\text{TiO}_2$  doping: cation-doping [32-41] and anion-doping [42-51]. Various studies have been performed to explain the band gap narrowing mechanism in  $\text{TiO}_2$  doping [30,42,52]. Nitrogen doping is the most used approach for obtaining visible light activity; [53-55] however, there is no established mechanism that explains the visible light activity of N-doped  $\text{TiO}_2$ . While some authors state that substitutional N-doping results in band gap narrowing due to the efficient mixing of orbitals 2p of N and O, others argue that band gap narrowing through modifications in the energy levels of valence and conduction bands can only occur with high concentrations of dopants and strong interactions among impurity energy states, valence and conduction bands [54]. Di Valentin and co-workers [56] based on the density functional theory (DFT) predicted that N atoms could occupy either substitutional or interstitial sites in the  $\text{TiO}_2$  lattice and thus generate localized energy states. When substitutional sites are occupied, a higher energy level extending the valence band is formed, while in the case of interstitial sites occupation, discrete energy levels above the valence band are created. Doping with other anions, such as carbon, can also show gap narrowing [57]. Some authors suggest that the use of doping agents results in modifications of (101)  $\text{TiO}_2$  surface [58]. These modifications can increase the transfer of photogenerated electrons to the outer surface regions, facilitating the photocatalytic reactions and improving the quantum efficiency of the photocatalytic processes.

Another approach used for obtaining visible light activity is metal ion doping. Some theories explain the visible light response obtained with this type of doping such as, the occurrence of band gap narrowing and intrinsic defects by either substitutional or interstitial substitution in the  $\text{TiO}_2$  matrix [54]. Metal ion doping induces, however, recombination of charge carriers lowering the overall efficiency of photocatalysis. Additionally, some reports point to differences in the photocatalytic phenomena under visible light and UV radiation. For UV radiation, as discussed in Section 2, both superoxide and hydroxyl radicals are produced. Nevertheless, for the

case of visible light activity, a less oxidative superoxide radical was suggested to be formed and being the main responsible for the photocatalytic activity [54,59,60]. Renguifo-Herrera and co-workers [59] developed N and S co-doped  $\text{TiO}_2$  presenting an intense visible-light absorption. However, its photocatalytic activity was low, similar to P25 under solar simulated light. These results can be ascribed to the fact that the photogenerated holes on the intermediary energy levels formed by N and S co-doping under visible light do not present sufficient redox potential to oxidize water and thus are not able to produce  $\text{OH}^\cdot$  radicals.

The main difference between doping and decoration is related to which part of the  $\text{TiO}_2$  is modified. In the case of doping, the modifications are conducted inside the crystalline structure of  $\text{TiO}_2$ , while in the case of decoration the modifications are made on the  $\text{TiO}_2$  surface. After excitation of  $\text{TiO}_2$ , electrons migrate to the attached decorating particle where they become trapped, minimizing the electron-hole recombination [61]. The migration of electrons to the decorating particles was confirmed in several studies [62-64], which showed an improved photocatalytic activity of the decorated  $\text{TiO}_2$  when compared to pristine  $\text{TiO}_2$ ; the holes migrate then to the semiconductor surface without recombining [62-64]. Few review articles analysing doping and decorating effects on photocatalysis have been published recently [65-68].

An effect that worth to be explained and that has been gathering interest in the scientific community is the surface plasmon resonance effect - SPR effect. When a metal nanoparticle is subjected to an oscillating electric field as the case of incident light, the free electrons in the nanoparticle will answer to that electric field also by oscillating. This behavior is called localized surface plasmon resonance and it can be adjusted by manipulating the size, shape and dielectric environment to change the interaction of the nanoparticles with incident light. Thus, it is possible to scatter the incident light with metal nanoparticles and increase the optical path of photons, leading to an absorption enhancement in certain wavelengths. SPR effect also promotes changes in the energy of the Fermi level caused by the electron storage effects in the metal nanoparticle [54]. Localized SPR of gold and silver nanoparticles normally results in strong and broad absorption bands in the visible light region, which can be exploited to attain visible light-activated photocatalysts [61,69-71].

Important to mention that one of the possible disadvantages of  $\text{TiO}_2$  decoration is the corrosion

and dissolution of decorating metal particles during the photocatalytic reaction [72]. The decorative particles can also act as co-catalysts, reducing the overvoltage of the redox reactions involved in photocatalysis. The use of co-catalysts allow a given electrochemical reaction to progress faster [73]. For instance, in photoelectrochemical water splitting, the lower level of the conduction band must be more negative than the redox potential of  $H^+/H_2$  (0 V vs. NHE, at pH = 0) and the top level of the valence band must be more positive than the redox potential of  $O_2/H_2O$  (1.23 V, at pH = 0). Since this reaction is very difficult to accomplish using  $TiO_2$  photocatalyst, the use of co-catalysts such as Pt, Au and Rh for  $H_2$  evolution [74] and  $RuO_2$  for  $O_2$  evolution [75] is essential.

## 2.2. $TiO_2$ /graphene composite

$TiO_2$  photoactivity can also be enhanced with the production of  $TiO_2$  composites. The most notable case is the production of  $TiO_2$ /graphene composites. In  $TiO_2$ /graphene composites, the electron-hole pairs are generated upon  $TiO_2$  excitation under UV light irradiation. These photogenerated electrons are then injected into graphene due to the more positive Fermi level of graphene [76]. The high carrier mobility of graphene accelerates excited electron transport that enhances the photocatalytic performance [77]. Simultaneously, Ti-O-C bonds formed in the  $TiO_2$ /graphene photocatalyst originate a red shift of few dozens of nanometers in the solar spectrum, reducing its bandgap and making it sensitive to longer-wavelength light [78,79]. The resulted photocatalyst presents then an extended photoresponse of up to ca. 440 nm

$TiO_2$  photooxidation is normally assigned intermediated free radicals  $OH^\cdot$  (oxidation potential of 2.8 V [80]) and  $O_2^\cdot^-$  (reduction potential of -0.137 V [81]), making necessary a thermodynamic minimum band gap of 2.94 eV for generating both radicals. Since most of band gap shortening approaches consider the creation of intermediate energy levels, cf. section 3, making the electron energy gain a stepwise process, the lowest and highest energy levels are still available. This means that, despite the band gap shortening below e.g. 2.8 eV, the photocatalyst is still active towards  $OH^\cdot$  and  $O_2^\cdot^-$  generation [82]. Nevertheless, the visible light activity of the  $TiO_2$ /graphene composites is not fully understood [83,84]. When graphene is bounded to  $TiO_2$  the overall photocatalytic performance is largely improved. This is mainly attributed to three effects: i) efficient charge separation and transportation; ii)

extended light absorption range; and iii) enhanced adsorptivity of the reactant species [79].

For photocatalytic indoor applications, such as for photoinactivation of microorganisms, a very promising photocatalyst is  $Au/TiO_2$ /graphene. The use of gold nanoparticles is expected to promote increased values of photoactivity due to the high surface plasmon resonance effect observed with these nanoparticles [61,85]. The  $Au/TiO_2$ /graphene, already described for the  $H_2$  production [86], shows enhanced photocatalytic activity due to the surface plasmon resonance effect of the Au nanoparticles, that broadens the visible light response of the  $TiO_2$ , and the excellent electron transport properties of graphene, which decreases the recombination of electron and hole pairs. Au nanoparticles, as explained before, can also reduce redox overpotentials [87].

## 3. PHOTOINACTIVATION

### 3.1. Rationale of using $TiO_2$ photocatalysis as the basis of new disinfection methods

The intensive use of antimicrobial agents, including antibiotics in human and veterinary chemotherapy, aquaculture and animal husbandry have been pointed out as the main cause behind the tremendous increase of antibiotic resistance in clinical settings and in the environment [88]. The emergence and spread of antibiotic resistant bacteria is not only of paramount public health concern, but it leads also to high costs for the national health services. Organic disinfectants are among the substances that may promote antibiotic resistance dissemination, given the occurrence of co-selection due to genetic linkage between antibiotics and biocides [89-92]. Therefore, the development of new disinfection techniques based on biocides naturally occurring in the human immune system is very attractive.

Phagocytic cells of the human immune system use the cytotoxic effects of ROS as a component of their host defence mechanism [93-95]. When a phagocyte encounters a microorganism, a portion of the phagocyte membrane surrounds it – the first step of a phagolysosome formation. This process leads to increased phagocyte oxygen consumption and activates a unique membrane-associated NADPH-dependent oxidase complex [96]. This enzymatic complex univalently reduces  $O_2$  to  $O_2^\cdot^-$ , which further dismutates to  $H_2O_2$  [96]. Another mecha-

nism involved in phagocyte-mediated oxidant generation and microbial toxicity involves the iron-catalysed intra- or extracellular reaction of  $O_2^{\cdot-}$  and  $H_2O_2$  to form  $OH^{\cdot}$  [94]. These ROS are known to be highly reactive with biological molecules and various authors proposed that  $OH^{\cdot}$  radical is the most toxic [97-100]. During the photocatalysis process similar ROS are formed. Hence, photoinactivation seems a good alternative to commonly used disinfection methods.

Matsunaga and co-workers in 1985 were the first authors assessing the feasibility of using UV-activated  $TiO_2$  for photoinactivation [7]. This study reported the successful photoinactivation of both Gram negative and Gram positive bacteria (*Escherichia coli* and *Lactobacillus acidophilus*, respectively) and yeasts (*Saccharomyces cerevisiae*) cells by a semiconductor powder (platinum-doped titanium dioxide, Pt- $TiO_2$ ). This pioneer work triggered numerous studies to assess the efficiency of  $TiO_2$  photocatalysis on the inactivation of microorganisms and viruses (Tables 1-3) as well as microbial toxins and prions [11,101]. A representative summary of the studies performed up to now on photoinactivation, as well as a comparison of this technique with traditional disinfection methods is given below.

### 3.2. Target test organisms and $TiO_2$ matrices

Given the commercial availability of  $TiO_2$  nanoparticles, most of the studies assessing the efficacy of photoinactivation have been carried out with P25 (Table 1), which shows high performance and stability when excited with UV radiation [102]. Most of the studies used axenic suspensions of bacteria as target organisms, being *Escherichia coli*, the well characterized and universally used faecal contamination indicator, the most used. However, domain *Bacteria* accommodates an immense diversity of organisms, reflected in a wide variety of phylogenetic, genotypic and phenotypic groups. Therefore, differences in cellular structure, metabolism, pathogenicity, or tolerance against stressful conditions, including resistance to antimicrobial agents, may influence the susceptibility of bacteria to photocatalysis. This explains why other bacteria, including Gram positive bacteria (phyla *Firmicutes* and *Actinobacteria*), endospore formers (a restricted group of *Firmicutes*, including genera such as *Bacillus* and *Clostridium*), pathogens or opportunistic pathogens (such as *Legionella pneumophila* and *Pseudomonas aeruginosa*), and antibiotic resistant bacteria have been used as test

organisms in photoinactivation trials (Table 1, [103-106]). Given the complexity of the bacterial communities in natural environments, some studies assessed the efficacy of photocatalysis in mixed suspensions of known composition, or in a more realistic way, in wastewater (Table 1). The efficacy of photocatalysis in the inactivation of eukaryotic microorganisms, both in axenic or mixed suspensions has also been assessed. In fact, the differences in the cellular structure of prokaryotic and eukaryotic organisms may lead to distinct tolerances to photocatalysis. Similar reasons are behind the studies performed with prokaryotic and eukaryotic dormant forms (spores, cysts). Indeed, the inactivation of these structures, particularly the bacterial endospores, has been a challenge due to their well-known resistance to chemical and physical antimicrobial agents [107,108].

$TiO_2$  photoinactivation is expected to be the basis of different processes and materials compatible with commercial applications for disinfection. Indeed, photocatalysis-based new disinfection processes can be potentially used in several fields, such as water disinfection [97,109-121], medical applications [119,122-125], and pharmaceutical and food industry [124]. Given the wide variety of potential applications, assessment of photoinactivation has been carried out in different matrices. The majority of the studies assessed the efficacy of  $TiO_2$  nanoparticles in aqueous suspension. This happens mainly because it is well known that the photoinactivation process is favored when cells are in direct contact with the photocatalyst. However, and primarily due to the potential harmful effects of nanoparticles in human health [126] and environment [127], immobilization of  $TiO_2$  has been studied (Tables 1-3). Indeed,  $TiO_2$  immobilization is very important for commercial applications [128], also due to two main reasons. Firstly, it is difficult to recover the photocatalyst when used as powder; this requires a post-treatment solid-liquid separation stage, which will add complexity and costs to the overall process [109]. Secondly, when it is not possible to recover the photocatalyst, the total loss of this material implies economical losses and it becomes itself a pollutant.

$TiO_2$  has been immobilized in different materials such as glass (plates, beads), polymers (polypropylene, polycarbosilane, cellulose acetate), paint and quartz disks [128-142]. These materials have been employed in surface coatings (glass, cellulose acetate sheets), paint coating and impregnated membranes. These approaches can be used for the inactivation of organisms in aqueous solu-

**Table 1.** Photoinactivation studies conducted under the influence of UV radiation (<380 nm).

Suspension type	Domain	Phylum	Organism	Initial cellular density (CFU/mL)	Photo catalyst	Photo-catalyst concentration (mg/L)	Irradiance (W/m <sup>2</sup> )	Contact time (min)	Reduction (%)	Type of Trial	Ref.
Axenic	Bacteria	Proteo-bacteria	Susceptible and multidrug resistant	10 <sup>3</sup> - 10 <sup>5</sup>	TiO <sub>2</sub> (P25, other commercial TiO <sub>2</sub> and produced TiO <sub>2</sub> )	62.5 and 125	4 and 8	5 to 80	99	Suspension	[106]
			<i>Acinetobacter baumannii</i>	10 <sup>6</sup> -10 <sup>7</sup>		100	55	40	99.9	Suspension	[116]
			Enterobacter cloacae								
			Susceptible and multiantibiotic resistant	10 <sup>3</sup> to 10 <sup>9</sup> , a,b		25 to 2500, c,d	2 to 1000, e,f,g	5 to 8640	99-100 (20 <sup>b</sup> )	Surface coating	[106, 116, 120, 131, 137, 141, 142, 156-159, 161, 165-169]
			<i>Escherichia coli</i>							Paint coating	[105]
				10 <sup>6</sup>		9000	10	40	98.7 -99	Paint coating	[116]
			<i>Salmonella typhimurium</i>	10 <sup>6</sup> -10 <sup>7</sup>		100	55	40	99.9	Suspension	[116]
			<i>Legionella pneumophila</i>	10 <sup>7</sup>		1000	1.65	1	100	Suspension	[162]
			<i>Pseudomonas aeruginosa</i>	10 <sup>3</sup> -10 <sup>7</sup>		1000-8 - 30, c,i	60 - 120	99.9 - 100	100	Surface coating	[120, 137, 141, 165]
						10000				Suspension	
			<i>Salmonella enteritidis</i>	10 <sup>7</sup>		1000	c	120	99.9	Suspension	[120]

a - 1.3 mg/mL, b - 1000 microbial cells (mc)/mL, c - 0.02% suspension of uncovered 100-nm TiO<sub>2</sub> nanoparticles, d - 15-25 mg of TiO<sub>2</sub> per disk, e - 3.42 x 10<sup>15</sup> Einsteins.s<sup>-1</sup>, f - 100 W high-pressure Hg lamp, g - 3900 lux, h - reduction in CO<sub>2</sub> mass balance, i - 2 x15 W, white light 356 nm peak emission, n.a. - not available

Suspension type	Domain	Phylum	Organism	Initial cellular density (CFU/mL)	Photo catalyst	Photo-catalyst concentration (mg/L)	Irradiance (W/m <sup>2</sup> )	Contact time (min)	Reduction (%)	Type of Trial	Ref.
Axenic	Bacteria	Proteo-bacteria	<i>Salmonella choleraesuis</i>	10 <sup>7</sup>		250 - 1250	1	180	> 99	Suspension	[170]
			<i>Vibrio parahaemolyticus</i>	10 <sup>7</sup>		250 - 1250	1	180	> 99	Suspension	[170]
		Firmicutes	<i>Bacillus anthracis</i>	10 <sup>3</sup> -10 <sup>6</sup>		1000, 1500	j	60, 90	4 <sup>k</sup>	Suspension	[171]
			<i>Bacillus cereus</i> endospores	10 <sup>5</sup>		250	34	540	> 5 <sup>k</sup>	Suspension	[160]
			<i>Bacillus subtilis</i>	10 <sup>5,1</sup>		d	74-318	8640	> 80, 20 <sup>h</sup>	Surface coating	[131, 136]
			<i>Bacillus subtilis</i> endospores	10 <sup>6</sup>		250	70	540	> 5 <sup>k</sup>	Impregnated Membrane Suspension	[160]
			<i>Geobacillus stearothermophilus</i> endospores	10 <sup>7</sup>	TiO <sub>2</sub> (P25, other commercial TiO <sub>2</sub> and produced TiO <sub>2</sub> )	50 to 1000	91±2	90	100	Suspension	[172]
			<i>Clostridium difficile</i> endospores	10 <sup>3</sup>		n.a.	30	300	3 <sup>a</sup>	Surface coating	[141]
			<i>Enterococcus hirae</i>	10 <sup>7</sup>		10 000	8	60	100	Suspension	[165]
			<i>Lactobacillus acidophilus</i>	10 <sup>7</sup>		n.a.	b	60	100	Surface coating	[173]
			<i>Listeria monocytogenes</i>	10 <sup>7</sup>		250 - 1250	1	180	> 99	Suspension	[170]

a- 15-25 mg of TiO<sub>2</sub> per disk, b - UVA - 9 W lamp; UVC -11 W lamp, c - log reduction, l - 1.5 mg/mL, d- UVA light, n.a. – not available

Suspension type	Domain	Phylum	Organism	Initial cellular density (CFU/mL)	Photo catalyst	Photo-catalyst concentration (mg/L)	Irradiance (W/m <sup>2</sup> )	Contact time (min)	Reduction (%)	Type of Trial	Ref.
Axenic	Bacteria	Firmicutes	Susceptible and Vancomycin-resistant <i>Enterococcus faecalis</i>	10 <sup>3</sup> -10 <sup>5</sup>		62.5 and 125	4 and 8	5 to 80	99	Suspension	[160]
			<i>Enterococcus faecium</i>	10 <sup>7</sup>		n.a.	c	n.a.	3 <sup>a</sup>	Surface coating	[137]
			<i>Staphylococcus aureus</i>	10 <sup>3</sup> -10 <sup>7</sup>		62.5 - 10 000	4 and 8	5 to 80	99 - 100	Suspension	[106, 161, 165, 167]
				10 <sup>5</sup>		n.a.	c	n.a.	>4 <sup>a</sup>	Surface coating	[137]
			Methicillin resistant <i>Staphylococcus aureus</i>	10 <sup>3</sup> -10 <sup>5</sup>		62.5 and 125	4 - 330	5 to 80	99	Suspension	[106]
			<i>Streptococcus sobrinus</i>	10 <sup>3</sup>		n.a.	30	80	99.8	Surface coating	[141]
			<i>Micrococcus luteus</i>	10 <sup>5</sup>		1000	d	3	5 <sup>a</sup>	Suspension	[174]
	Actino-bacteria		<i>Micrococcus luteus</i>	h		e	104	8640	20 <sup>f</sup>	Surface coating	[131]
	Bacteroidetes		<i>Bacteroides fragilis</i>	10 <sup>7</sup>		10 000	8	60	100	Suspension	[165]
	Cyano-bacteria		<i>Anabaena Microcystis</i>	n.a.		n.a.	6 and 43	60	100 <sup>g</sup>	Surface coating	[138]

a - log reduction, b - 2 x 15 W, white light 356 nm peak emission, c - UV light (300-400 nm, peak emission: 352 nm), d - 15-25 mg of TiO<sub>2</sub> per disk, e - reduction in CO<sub>2</sub> mass balance, f - relative <sup>14</sup>C-assimilation, g - 1.77 mg/mL, n.a. - not available

**Table 1 (Continuation).** Photoinactivation studies conducted under the influence of UV radiation (<380 nm).

Suspension type	Domain	Phylum	Organism	Initial cellular density (CFU/mL)	Photo catalyst	Photo-catalyst concentration (mg/L)	Irradiance (W/m <sup>2</sup> )	Contact time (min)	Reduction (%)	Type of Trial	Ref.
Axenic	Eukarya	Ascomycota	<i>Candida albicans</i>	10 <sup>3</sup> -10 <sup>5</sup>	TiO <sub>2</sub> (P25, other commercial)	20 (n.a.)	315 and 330, <sup>a</sup>	30, n.a.	96 (1.2 <sup>b</sup> )	Suspension Surface coating	[137, 161]
			<i>Aspergillus niger</i> spores	<sup>c</sup>	TiO <sub>2</sub> and produced	<sup>d</sup>	104	8640	0 <sup>e</sup>	Surface coating	[131]
			<i>Fusarium</i> (5 different strains)	10 <sup>3</sup>	TiO <sub>2</sub>	35	34	360	3 <sup>b</sup>	Suspension	[175]
			<i>Penicillium citrinum</i>	10 <sup>5</sup>		n.a.	74 and 318	n.a.	< 60	Impregnated membrane	[136]
		Apicomplexa	<i>Cryptosporidium parvum</i>	Variable		n.a.	100	Variable	100	Impregnated membrane	[134]
		Stramenopiles	<i>Melosira piles</i>	n.a.		n.a.	6 and 43	60	60 <sup>f</sup>	Surface coating	[138]
		Metamonada	<i>Giardia lamblia</i>	10 <sup>5</sup>		<sup>g</sup>	24 and 100	60	100	Surface coating	[134, 176]

a - 2 x15 W, white light 356 nm peak emission, b - log reduction, c - 0.6 mg/mL, d - 25 mg of TiO<sub>2</sub> per disk, e - reduction in CO<sub>2</sub> mass balance, f - relative <sup>14</sup>C-assimilation, g - 3 % colloidal solution, n.a. - not available.

**Table 1 (Continuation).** Photoinactivation studies conducted under the influence of UV radiation (<380 nm).

Suspension type	Domain	Phylum	Organism	Initial cellular density (CFU/mL)	Photo catalyst	Photo-catalyst concentration (mg/L)	Irradiance (W/m <sup>2</sup> )	Contact time (min)	Reduction (%)	Type of Trial	Ref.		
Mixed	Bacteria	Proteo-bacteria	<i>Escherichia coli</i>	10 <sup>5</sup>	TiO <sub>2</sub> (P25, other)	25 <sup>b</sup>	<sup>c</sup>	90	5.5 <sup>a</sup>	Surface coating	[135]		
			<i>Pseudomonas aeruginosa</i>	10 <sup>4</sup>	commercial TiO <sub>2</sub> and produced TiO <sub>2</sub> )		120	5 <sup>a</sup>					
	Eukarya	Firmicutes	<i>Bacillus subtilis</i> endospores	10 <sup>6</sup>				480	1.7 <sup>a</sup>				
			<i>Acanthamoeba</i>	10 <sup>4</sup>			120	4 <sup>a</sup>					
			<i>Polyphaga</i> (Trophozoites)	10 <sup>4</sup>			480	0					
			<i>Polyphaga</i> (Cysts)	10 <sup>4</sup>			240	5.4 <sup>a</sup>					
	Wastewater	Bacteria	Proteo-bacteria	<i>Candida albicans</i>	10 <sup>5</sup>				240	5.5 <sup>a</sup>			
				<i>Fusarium solani</i> (Conidia)	10 <sup>5</sup>			240	5.5 <sup>a</sup>				
			Firmicutes	<i>Escherichia coli</i>	Variable		100	38		360	100	Suspension	[177]
				<i>Enterococcus faecalis</i>	n.a.		250	<sup>d</sup>		180	99.6	Impregnated membrane	[143]
-	Proteo-bacteria	Total coliforms	10 <sup>4</sup> - 10 <sup>7</sup>		0.2 - 2000	1.5 (n.a.), <sup>e</sup>	3 - 150	100	Suspension	[121, 178-180]			
		Total heterotrophic bacteria	10 <sup>4</sup>		5000	<sup>f</sup>		360	100	Suspension	[118]		

a - log reduction, b - mg/cm<sup>2</sup>, c - 70 W/m<sup>2</sup> in the 300 nm–10 mm range, 200W/m<sup>2</sup> in the 300–400nm UV range, d - 800 W UV lamp, e - 36 W UV Lamp, f-Photon flux: 0.2 mmol/h < 280 nm, 18 mmol/h 280±315 nm, 390 mmol/h 315±380 nm or 5 mmol/h < 280 nm, 150 mmol/h 280±315 nm, 220 mmol/h 315±380 nm, n.a. – not available

**Table 2.** Photoactivation studies conducted under the influence of UV radiation (<380 nm) with TiO<sub>2</sub> modified photocatalysts. The modification types are: doping (x-TiO<sub>2</sub>) and decoration (x/TiO<sub>2</sub>).

SSuspension type	Domain	Phylum	Organism	Initial cellular density (CFU/mL)	Photo catalyst	Photo-catalyst concentration (mg/L)	Irradiance (W/m <sup>2</sup> )	Contact time (min)	Reduction (%)	Type of Trial	Ref.			
Axenic	Bacteria	Proteo-bacteria	<i>Escherichia coli</i>	10 <sup>9</sup>	Ag/TiO <sub>2</sub>	1000	0.5	35	6 <sup>a</sup>	Suspension	[181]			
			<i>Bacillus cereus</i> endospores	10 <sup>4</sup> - 10 <sup>5</sup>	Ag-TiO <sub>2</sub>	n.a.	50	1440	100	Surface coating	[132]			
				<i>Staphylococcus aureus</i>	10 <sup>9</sup> - 10 <sup>10</sup>	Fe <sub>3</sub> O <sub>4</sub> @TiO <sub>2</sub> <sup>b</sup>	2500	4	20	93	Suspension	[182]		
			<i>Streptococcus pyogenes</i>							96				
			<i>Staphylococcus saprophyticus</i>						99.5					
			<i>Lactococcus lactis</i>	10 <sup>4</sup>				150	10	99.98	Surface coating	[133]		
			Proteo-bacteria	Firmicutes	<i>Pseudomonas fluorescens</i>									
					<i>Escherichia coli</i>	10 <sup>3</sup>				60 and 120	100	Suspension	[7]	
			Eukarya	Ascomycota	Chlorophyta	<i>Lactobacillus acidophilus</i>						100		
						<i>Saccharomyces cerevisiae</i>						100		
<i>Chlorella vulgaris</i>										45				
<i>Tetraselmis suecica</i>	10 <sup>3</sup>								60	100	Suspension	[183]		
<i>Amphidinium carterae</i>														

a -log reduction, b - core/shell magnetic nanoparticles, c -300-W xenon lamp, a 400-W metal halide lamp and a 500-W white fluorescent lamp, d - 20 W A-type UV lamps, n.a. - not available.

**Table 3.** Photoinactivation studies conducted under the influence of visible light (>380 nm) with TiO<sub>2</sub> modified photocatalysts.

SSuspension type	Domain	Phylum	Organism	Initial cellular density (CFU/mL)	Photo catalyst	Photo-catalyst concentration (mg/L)	Irradiance (W/m <sup>2</sup> )	Contact time (min)	Reduction (%)	Type of Trial	Ref.		
Axenic	Bacteria	Proteobacteria	<i>Escherichia coli</i>	10 <sup>2</sup> -10 <sup>9</sup>	Ag/C-TiO <sub>2</sub> , AgBr/TiO <sub>2</sub> , I-TiO <sub>2</sub> , PdO-TiO <sub>2</sub> , CNT-doped TiO <sub>2</sub> , N-TiO <sub>2</sub> , C-TiO <sub>2</sub> , Pt-TiO <sub>2</sub> , S-TiO <sub>2</sub> , N-F-TiO <sub>2</sub> , Mn-TiO <sub>2</sub> , Co-TiO <sub>2</sub> , Fe-TiO <sub>2</sub> , Mn/Co-TiO <sub>2</sub> , Cathecol/TiO <sub>2</sub> , TiO <sub>2</sub> /Graphene	10-1000, <sup>a</sup> 1100, 3900 - 15 000 <sup>b, c, d, e</sup>	1.31 × 10 <sup>12</sup> - 1100, 3900 - 15 000 <sup>b, c, d, e</sup>	15-1440, <sup>f</sup>	100	Impregnated Membrane Suspension Surface coating	[128, 129, 139, 140, 184, 186-197]		
					<i>Erwinia</i>	10 <sup>4</sup> -10 <sup>5</sup>	Synthesized TiO <sub>2</sub>	n.a.	724 <sup>b</sup>	20-60	> 90	Thin films	[130]
					<i>Carotovora</i>	10 <sup>4</sup> -10 <sup>5</sup>	Synthesized TiO <sub>2</sub>	n.a.	724 <sup>b</sup>	20-60	> 90	Thin films	[130]
					<i>Enterobacter cloacae</i>	10 <sup>4</sup>	C-TiO <sub>2</sub>	200	100 and 900	5	> 80	Suspension	[185]
					<i>Shigella flexneri</i>	10 <sup>2</sup> - 10 <sup>8</sup>	Mn-TiO <sub>2</sub> , Co-TiO <sub>2</sub> , Mn/Co-TiO <sub>2</sub>	25-250	1.31 × 10 <sup>12</sup>	60	100	Suspension	[191]
					<i>Klebsiella pneumoniae</i>	10 <sup>4</sup> - 10 <sup>5</sup>	C-TiO <sub>2</sub> , Pt-TiO <sub>2</sub>	50, 200	100 - 900	5, 75	< 90	Suspension	[185, 198]
					<i>Acinetobacter baumannii</i>	10 <sup>3</sup> -10 <sup>8</sup>	P25, PdO-TiO <sub>2</sub> , C-TiO <sub>2</sub> , AgBr/TiO <sub>2</sub> , Pt-TiO <sub>2</sub> , Cathecol/TiO <sub>2</sub>	50 - 200, <sup>c</sup>	10 - 900	5 - 1440	100	Paint coating Surface coating	[129, 140, 185, 190, 193, 198]
					<i>Staphylococcus aureus</i>	10 <sup>5</sup>	Pt-TiO <sub>2</sub>	50	480	75	> 90	Suspension	[198]
					<i>Streptococcus pyogenes</i>	10 <sup>5</sup>	Pt-TiO <sub>2</sub>	50	480	75	> 90	Suspension	[198]

		<i>Enterococcus faecalis</i>	$10^6$ - $10^9$	Ag/C-TiO <sub>2</sub> , N-TiO <sub>2</sub> , C-TiO <sub>2</sub>	1000	450-500, 15 000 <sup>b</sup>	300	4 <sup>g</sup>	Suspension Surface coating	[139, 184]
<i>Eukarya</i>	Ascomy- cota	<i>Saccharomyces cerevisiae</i>	$10^2$	PdO-TiO <sub>2</sub>	n.a.	100	180	65	Thin films	[140]
		<i>Aspergillus niger</i> spores	$10^2$	PdO-TiO <sub>2</sub>	n.a.	100	480	0	Thin films	[140]

a - 2 wt.% in paint, b - lux, c - 4 x 24 W fluorescence lamps, d - portion of UV (290–400 nm) of 0.05–0.12 W m<sup>-2</sup> intensity, and visible light (400–700 nm) with a range of intensity 2.70–3.99 W m<sup>-2</sup>, e - UVA - 3 mW/cm<sup>2</sup> (SSL) VL-162 370 lux, f - months of May-September in Tehran (IRAN) at around noon, g - log reduction, n.a. - not available.

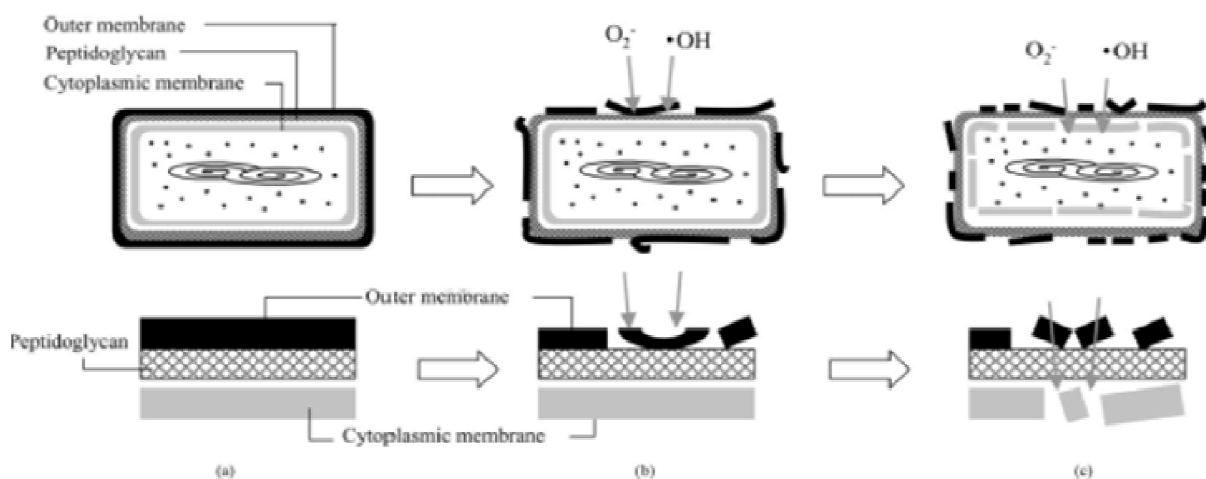


**Fig. 2.** Free radicals mode of action (reprinted with permission from M. Dizdaroglu, P. Jaruga, M. Birincioglu and H. Rodriguez // *Free Radical Biol. Med.* **32** (2002) 1102. (c) 2002 Elsevier).

tions (e.g. reactor wall), air (e.g. air filters) and fomites (e.g. paint coating). In the specific case of water treatment, the advantage of using coated glass beads is the larger specific surface area, which allows a more efficient photoinactivation of microorganisms. However, the use of glass beads can increase the cost and complexity of the process. In impregnated membranes,  $\text{TiO}_2$  is deposited in the interstices of the membrane, improving the surface contact area between  $\text{TiO}_2$  and the microorganisms. This method seems to be useful for wastewater treatment [143] but can also be used for the photoinactivation of air microorganisms [136]. Paint coating seems to be, currently, the most promising immobilization matrix for commercial applications. Paint is a readily available material, easy to be applied onto surfaces and does not react with the photocatalyst nor interfere with the photocatalytic efficiency [144]. Furthermore, paint provides a good support for the photocatalyst in a 3D arrangement and can be applied in hospitals and other buildings where infections should be prevented.

### 3.3. Photoinactivation mechanism

To better understand the effect of  $\text{TiO}_2$  photocatalysis on the differential inactivation of the cells and thereof dormant forms, the mechanism of action of photoinactivation is summarized as follows. All the cellular constituents, such as polysaccharides, lipids, proteins and nucleic acids can be attacked by ROS formed during photocatalysis. However, cell wall is the initial target for the photocatalytic attack. Considering as example the Gram-negative bacteria, the oxidation of components of the outer membrane by ROS promotes an increase in cell perme-

ability. Consequently, ROS easily reach the cytoplasmic membrane, where peroxidation of membrane lipids also occurs. The consequent structural and functional disorders of the cytoplasmic membrane lead to ROS entrance in the cell, where they negatively interfere with DNA replication [11,145] and respiratory activity [7,146] due to the direct oxidation of coenzyme A into its dimeric form. Ultimately, ROS attack leads to the loss of cell viability and cell death [147-149]. The initial process of *E. coli* photoinactivation by the action of  $\text{TiO}_2$  photocatalysis is depicted in Fig. 2. Evidences indicate that the  $\text{TiO}_2$  photocatalytic reaction results in continued bactericidal activity, well after the UV illumination terminates [148].

In what concerns Gram-positive bacteria, the majority of the studies showed that they are more resistant to photocatalytic inactivation than Gram-negative [11]. However, some authors reported opposite observations [141,150,151]. Some of the differences encountered in the susceptibility to photoinactivation between Gram-negative and Gram-positive bacteria may be caused by the experimental conditions. For instance, van Grieken and co-workers [152] showed that the susceptibility of *E. coli* and *Enterococcus faecalis* to photocatalysis in natural waters was similar, whereas in distilled water the Gram-positive was more resistant. Nevertheless, the different cell wall structure of Gram-negative and positive bacteria is actually cited as the main reason for the distinction on ROS attack susceptibility. Gram-negative bacteria have a triple-layer, with an inner cytoplasmic membrane, and a cell wall composed by a thin peptidoglycan layer and an outer membrane. Besides the inner cyto-

plasmic membrane, the Gram-positive bacteria have a thick peptidoglycan layer. The high porosity of peptidoglycan allows solutes, such as ROS, to permeate. Therefore, also Gram-positive cells become susceptible to radical attack [153,154]. However, the thickness of the peptidoglycan layer in these bacteria may allow a delay in the loss of cell permeability, and/or retard oxidants diffusion to vital sites. Indeed, both mechanisms would explain the higher resistance of Gram-positive bacteria to TiO<sub>2</sub> photoinactivation when compared with Gram-negative ones. On the other hand, the presence of an outer membrane in Gram-negative cells may explain why under certain circumstances these bacteria are more resistant to ROS attack than Gram-positive cells [7,141,150]. The rigid cell wall of filamentous and unicellular fungi, composed mainly of soluble and insoluble polysaccharide polymers, make them more resistant to ROS attack than bacterial cells [11,135]. Generally, dormant forms, such as fungal spores [131], cysts [135], and bacterial endospores [131], are even more resistant than the vegetative cells which proves the role of cell wall thickness and complexity in ROS defence.

### 3.4. Efficiency of photoinactivation

In this section, a summary of the studies carried out on the efficiency of photoinactivation under UV and visible radiation is given. Given the high number of studies published up to now in this field, a selection was made. The selection criteria included the type of tested microorganism, light sources and testing conditions, and the utilization of novel TiO<sub>2</sub> based photocatalysts. A more extensive literature review on this topic can be found elsewhere [11].

The factors affecting cell death, caused by an antimicrobial agent, include the agent concentration, time of exposure, and type and density of cells. Therefore, for a rigorous comparison of efficiency among antimicrobial agents and/or type of target organisms, standardized methods should be used. Even though there is already a standard for testing photocatalytic materials [155], most studies does not follow this standard, probably because this standard is referred to surfaces and most of studies are based on the use of suspensions, as previously mentioned. Hence, it is very difficult to compare the photoinactivation efficiency against different target organisms in different conditions, even when the same photocatalyst (e.g., P25) is used (Tables 1-3). For example, studies reporting the inactivation of *E. coli* in suspension used photocatalyst concentrations ranging from 50 to 1000 mg/L, values of

UV irradiance from 2 to 1000 W/m<sup>2</sup>, time of contact from 5 min up to 144 h, and cell densities ranging between 10<sup>3</sup> to 10<sup>7</sup> colony forming units (CFU)/mL. In addition, different strains of this species were used ([105,106,116,120,131,137,141,156-159], Table 1). Nevertheless, most of the studies performed up to now included controls and, in some cases, the inactivation of different organisms or matrices were tested under the same conditions allowing a better comparative assessment and thus valuable data to conclude on the efficacy of photoinactivation.

#### 3.4.1. UV-TiO<sub>2</sub> photoinactivation

Photocatalytic experiments under UV radiation produce high levels of photoinactivation for the majority of the different microorganisms tested. As mentioned previously, P25 has been the most used photocatalyst. However, synthesized, pristine, doped or decorated TiO<sub>2</sub> were also reported.

As referred to above, despite the difficulties encountered on comparing the results obtained in the different studies shown in Tables 1 and 2, some conclusions can be drawn. UV-TiO<sub>2</sub> photocatalysis seems to be effective on the inactivation of all the types of microorganisms. Studies carried out by Herrera Mélian *et al.* [143], Dillert *et al.* [118] and Rincón *et al.* [121] should be highlighted since high values of inactivation of total heterotrophic bacteria and coliforms were reported for real wastewater samples.

But care must be taken to define the operating conditions since organisms with different cellular structure and complexity, such as *E. coli*, *Bacillus subtilis* endospores and the yeast *Candida albicans*, have very different susceptibility to photoinactivation. Total inactivation of *E. coli* cellular at a density of 10<sup>6</sup> CFU/mL was achieved within 40 minutes of contact in suspension, with a photocatalyst concentration of 0.1 g/L and irradiance of 55 W/m<sup>2</sup> [116]. However, to completely inactivate *Bacillus subtilis* endospores at a similar initial spore density (10<sup>6</sup> spore/mL), a photocatalyst concentration of 0.25 g/L, an irradiance of 70 W/m<sup>2</sup> and 540 minutes were needed [160]. Despite of shorter time of contact (30 minutes) and photocatalyst concentration (0.02 g/L) a very high irradiance value (330 W/m<sup>2</sup>) was necessary to achieve 96% inactivation of *Candida albicans* at and initial cellular density of 10<sup>3</sup> CFU/mL [161]. On the contrary, pathogenicity seems to have less influence on bacterial susceptibility against photoinactivation. For example, Cheng *et al.* [162] reported that total inactivation of pathogenic *Legionella pneumophila* serotype 1 at an ini-

tial cellular density of  $10^7$  CFU/mL was attained after 105 minutes with a photocatalyst concentration of 0.2 g/L and an irradiance of  $1.65 \text{ W/m}^2$ , conditions comparable to the ones used by Ibañez et al. [116] for the photoinactivation of *E. coli*.

Some antibiotic resistant bacteria are also susceptible to  $\text{TiO}_2$  photocatalytic inactivation. Photoinactivation values of susceptible and antibiotic resistant strains of *E. coli* [105] and *S. aureus* (MRSA) [106] were not significantly different (Table 1). However, differences between antibiotic resistant and sensitive counterparts have also been reported [106]. A multidrug-resistant *Acinetobacter baumannii* (MDRAB) was ca. 2 times more susceptible to photoinactivation than the antibiotic sensitive *Acinetobacter baumannii* control strain. Opposite results were obtained for *Enterococcus faecalis*, where the vancomycin resistant strain (VRE) showed ca. 2 times less susceptibility against photoinactivation than the susceptible strain [106]. Indeed, different susceptibility against oxidative stress was already reported among strains of the same microbial species [163,164]. Hence, despite the utmost importance of comparing the response of a wide variety of these organisms against photoinactivation, to the best of our knowledge, such studies were not reported yet.

Even though efficient, high photocatalyst concentrations, powerful light sources or high contact times are needed when P25 or other synthesized pristine  $\text{TiO}_2$  are used. Thus, in order to achieve higher photoinactivation performances with less severe conditions, modified titanium dioxide (doped and/or decorated) has been studied (Table 2). As discussed in detail in Section 3, these  $\text{TiO}_2$  modifications enhance the photocatalytic activity of the photocatalyst. Much lower irradiance ( $0.5$  versus  $55 \text{ W/m}^2$ , respectively) and lower contact times (35 versus 40 minutes) were necessary to achieve total inactivation of *E. coli* at a higher cellular density ( $10^9$  versus  $10^6$  CFU/mL, respectively) with a  $\text{TiO}_2$  decorated with silver nanoparticles [181] compared with pristine  $\text{TiO}_2$  [116]. However, a final conclusion concerning the performance of the modified photocatalyst cannot be retrieved because a 10 times higher concentration of  $\text{TiO}_2$  decorated with Ag (1 g/L) [181] than of pristine  $\text{TiO}_2$  [116] was used. Nevertheless, other studies suggest that modification of the photocatalyst improve, in fact, their inactivation performance. For the complete inactivation of *S. aureus* at an initial cellular density of  $10^6$  CFU/mL, 10 g/L of synthesized pristine  $\text{TiO}_2$  and irradiance of  $8 \text{ W/m}^2$  for 60 minutes were necessary [165], while 2.5 g/L of  $\text{Fe}_3\text{O}_4$  decorated  $\text{TiO}_2$  and an

irradiance of  $4 \text{ W/m}^2$  for 20 minutes were sufficient to inactivate 93 % of *S. aureus* viable cells at an initial higher concentration ( $10^9$  CFU/mL).

### 3.5. Visible light- $\text{TiO}_2$ photoinactivation

Despite the success of UV-photocatalysis in disinfection, the mutagenic action of this type of radiation hampers its use in the majority of the indoor spaces [113]. On the other hand, the negligible UV irradiance under common internal lighting conditions prevents the use of pure photocatalytic  $\text{TiO}_2$  in indoor spaces. Even in outdoor events, the low fraction of solar UV compared to the total solar irradiation advises the use of visible light photocatalysts. To overcome this major drawback, several studies focused on the development of modified titanium dioxide with enhanced visible light photoactivity have been conducted, as mentioned in Section 3.

Among the modified photocatalysts tested up to now, carbon doped  $\text{TiO}_2$ , decorated [184] or not [185] with silver nanoparticles was shown to respectively fully inactivate *E. coli* and *S. aureus* under visible light. Also manganese-, cobalt doped or co-doped Mn/Co- $\text{TiO}_2$  was shown to fully inactivate *Klebsiella pneumonia* [100]. As mentioned in Section 4, the use of graphene for photocatalytic applications by Akhavan *et al.* [186] resulted in a novel graphene oxide/ $\text{TiO}_2$  composite with an increased antibacterial activity under solar light irradiation when compared to bare  $\text{TiO}_2$  (roughly 7.5 times more).

Nevertheless, the disinfection performance of modified  $\text{TiO}_2$  under visible light is still lower than under UV radiation. Indeed, the inactivation fraction of vegetative cells of a wide variety of microorganisms under UV irradiation varies between 96% and 100% (Table 1), while under visible light ranges from 65% to 90% (Table 3). Moreover, to attain these inactivation values extreme conditions were necessary, i.e, very high values of irradiance (up to 15 000 lux), photocatalyst concentration (1 g/L) and/or contact time (1440 minutes). Finally, inactivation of dormant forms such as spores of *Aspergillus niger* under visible light was also not attained yet (Table 3).

Thus, optimization of photoinactivation under visible light envisaging a future commercial application of this technique is still needed.

### 3.6. Traditional disinfection methods

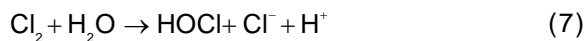
Traditional disinfection methods are based on the utilization of heat, radiation or chemical compounds.

Chlorine, hydrogen peroxide, ozone, and UV radiation are amongst the most used agents currently used to disinfect water, air or fomites. The disinfection methods based on each of these antimicrobial agents will be briefly overviewed next.

### 3.6.1. Chlorination

Chlorination as a disinfection technique is mainly based on the use of gaseous chlorine and/or hypochlorite. Chlorine gas ( $\text{Cl}_2$ ) is the elemental form of chlorine at standard temperature and pressure. Chlorine gas is approximately 2.5 times heavier than air and is highly toxic. Hypochlorite ( $\text{ClO}^-$ ) is usually obtained from sodium hypochlorite and calcium hypochlorite [199].

Chlorine gas hydrolyzes in water according to the following reaction (Eq. (7)):



while hypochlorous acid, resulting from the previous reaction, is a weak acid, which dissociates in aqueous solution:



Under typical water treatment conditions in the pH range 6–9, hypochlorous acid and hypochlorite are the main chlorine species. Depending on the temperature and pH level, different distributions of aqueous chlorine species ( $\text{Cl}_2$ , HOCl, and  $\text{ClO}^-$ ) are observed [200]. In addition to these major chlorine species, other chlorine intermediates including trichloride ( $\text{Cl}_3^-$ ) and chlorine hemioxide ( $\text{Cl}_2\text{O}$ ) can also be formed – Fig. 3. In solution, ratios of these intermediates are a function of temperature, pH and chloride concentration. Under typical water treatment conditions, the concentrations of  $\text{Cl}_3^-$  and  $\text{Cl}_2\text{O}$  are very low, accounting, at most, to 20% of all the chlorine species in solution [200,201].

Chlorination as a water disinfection method was first introduced in 1902 in Middlekerke, Belgium [202]. Chlorination is mainly used in water disinfection, however, hypochlorite is also used for the disinfection of some surfaces (mostly for countertops and floors), mainly in health care facilities [203]. A leading advantage of chlorination is that it is effective against a wide variety of bacteria and viruses. However, it cannot inactivate all microbes, being some protozoan cysts resistant to the effects of chlorine [204]. In cases where protozoan cysts are not a major concern, chlorination seems to be a good water disinfection method because it is inexpensive.

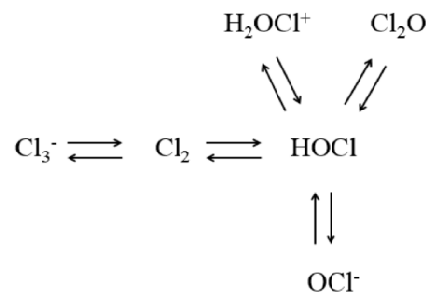


**Fig. 3.** Equilibrium of chlorine and its derivatives in solution at 25 °C (adapted from [196]).

The precise mechanism by which microorganisms are inactivated by chlorine has not yet been fully explained. However, some studies show that the bacterial cell membrane changes its permeability in the presence of chlorine [205,206]. The presence of suspended solids influences the action of chlorine because the particles and organic compounds usually provide protection to microorganisms. This protection usually comes from stabilization of the cell membranes, which reduces the access of chlorine to key cellular components for inactivation [206]. Indeed, microbial aggregates or microorganisms attached to or embedded in particles have been shown to have increased resistance to inactivation by chlorine, when compared to non-attached, free-swimming microorganisms. Dietrich and co-workers [206] reported, however, that chlorine is capable of penetrating particles in wastewater by radial diffusion. Greater chlorine penetration into wastewater particles was observed with increasing initial chlorine concentration, indicating that chlorine application could be tailored to penetrate particles of known size in order to achieve inactivation [206].

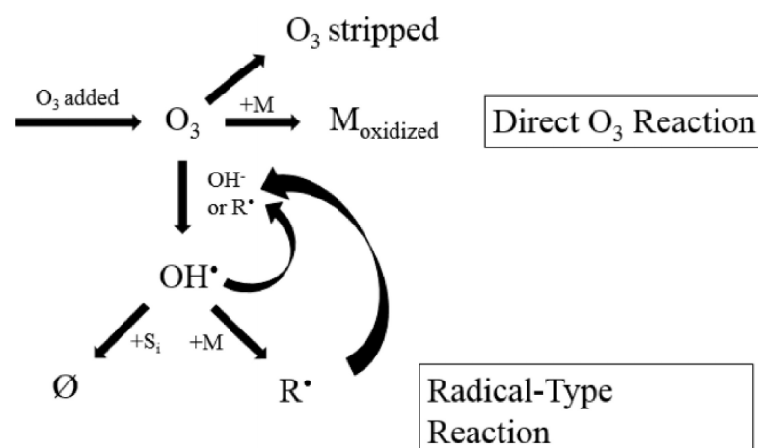
Some of the studies reported in the literature on the efficiency of chlorination on disinfection are summarized in Table 4. Koivunen and co-workers [207] studied the chlorination of *Enterococcus faecalis*, *Escherichia coli*, and *Salmonella enteritidis* in aqueous solution. In this work, concentrations of chlorine of 12 mg/L with a contact time of 10 minutes were used in order to achieve a log reduction value of around 3 for *Enterococcus faecalis*. But, even with a higher chlorine concentration (18 mg/L), lower reduction values were registered for *Escherichia coli* and *Salmonella enteritidis* (0.3 and 0.44, respectively) for the same contact time, demonstrating that microorganisms have distinct tolerance against chlorination. In wastewater samples, Hassen and co-workers [208] registered log reduction values up to 3.7 and 4.4 for fecal coliforms and enterococci, re-

Table 4. Inactivation of several microorganisms by chlorination.

Domain	Phylum	Organism	Type of suspension	Type of Trial	Chlorine concentration (mg/l)	Contact time (min)	Final chlorine concentration (mg/L)	Initial cellular density (CFU/mL)	Reduction (log)	Reference	
Bacteria	Firmicutes	<i>Clostridium perfringens</i> Spores	Axenic	Suspension	5	1440	n.a.	10 <sup>4</sup>	4	[209]	
		<i>Enterococci</i>	Wastewater	Suspension	6.5-25	15-40	1.2-3	10 <sup>4</sup> -10 <sup>5</sup>	4.5(99 <sup>a</sup> )	[208,210]	
		<i>Enterococcus faecalis</i>	Wastewater	Axenic	Suspension	8-30	30	0.2-0.3	10 <sup>5</sup> -10 <sup>7</sup>	5	[211,212]
		<i>Staphylococcus aureus</i>	Axenic	Suspension	1-5	30	30	0.5-3	10 <sup>8</sup> -10 <sup>9</sup>	b	[207]
		<i>Enterococcus faecalis</i>	Axenic	Suspension	1-5	30	30	0.5-3	10 <sup>8</sup> -10 <sup>9</sup>	b	[207]
		<i>Campylobacter jejuni</i>	Axenic	Suspension	0-4	120	120	n.a.	10 <sup>3</sup> -10 <sup>4</sup>	99 <sup>a</sup>	[213]
		<i>Citrobacter freundii</i>	Axenic	Suspension	0-10	120	120	n.a.	10 <sup>3</sup> -10 <sup>4</sup>	99 <sup>a</sup>	[213]
		<i>Enterobacter agglomerans</i>	Axenic	Suspension	0-10	120	120	n.a.	10 <sup>3</sup> -10 <sup>4</sup>	99 <sup>a</sup>	[213]
		<i>Enterobacter cloacae</i>	Axenic	Suspension	0-10	120	120	n.a.	10 <sup>3</sup> -10 <sup>4</sup>	99 <sup>a</sup>	[213]
		<i>Escherichia coli</i>	Axenic	Suspension	1-30	2.5-120	2.5-120	0.2-3	10 <sup>5</sup> -10 <sup>9</sup>	>5 (99 <sup>a</sup> ) <sup>b</sup>	[169,207, 211-213]
		<i>Fecal coliforms</i>	Wastewater	Suspension	6.5-25	15-5760	15-5760	1.2-3	10 <sup>4</sup> -10 <sup>6c</sup>	7 (99 <sup>a</sup> )	[208,210, 214]
		<i>Klebsiella oxyfoca</i>	Axenic	Suspension	0-10	120	120	n.a.	10 <sup>3</sup> -10 <sup>4</sup>	99 <sup>a</sup>	[213]
		<i>Klebsiella pneumoniae</i>	Axenic	Suspension	0-10	120	120	n.a.	10 <sup>3</sup> -10 <sup>4</sup>	99 <sup>a</sup>	[213]
		<i>Legionella gormanii</i>	Axenic	Suspension	0-4	120	120	n.a.	10 <sup>3</sup> -10 <sup>4</sup>	99 <sup>a</sup>	[213]

<i>Pseudomonas aeruginosa</i>	Axenic	Suspension	1 - 5	30	0.5-3	10 <sup>8</sup> -10 <sup>9</sup>	b	[207]
<i>Salmonella enterica</i>	Axenic	Suspension	0-4	120	n.a.	10 <sup>3</sup> -10 <sup>4</sup>	99 <sup>a</sup>	[213]
<i>Salmonella enteritidis</i>	Axenic	Suspension	18	n.a.	0.2-0.3	10 <sup>5</sup> -10 <sup>7</sup>	0.5	[212]
<i>Shigella sonnei</i>	Axenic	Suspension	0-4	120	n.a.	10 <sup>3</sup> -10 <sup>4</sup>	99 <sup>a</sup>	[213]
Total coliforms	Wastewater	Suspension	11-21	15-5760	n.a.	c	7(99 <sup>a</sup> )	[210,241]
<i>Yersinia enterocolitica</i>	Axenic	Suspension	0 -4	120	n.a.	10 <sup>3</sup> -10 <sup>4</sup>	99 <sup>a</sup>	[213]
<i>Cryptosporidium parvum</i>	Axenic	Suspension	5	1440	n.a.	10 <sup>4</sup>	4	[209]
<i>Eukarya</i>	<i>Apicomplexa</i>							

a -%, b – evaluated through the consumption of chlorine and presence of residual chlorine, c- 1 million to 20 millions per 100 ml, n.a. – not available.



**Fig. 4.** Mechanisms involved in the ozonation process. In the figure, M is referred to the solute, M<sub>oxid</sub> to the oxidized solute, S<sub>i</sub> to the free radical scavenger, Ø to products that do not catalyze the ozone decomposition and R to the free radicals that catalyze the ozone decomposition. (Reprinted with permission from J. Koivunen and H. Heinonen-Tanski // *Water Res.* **39** (2005) 1519. (c) 2005 Elsevier).

spectively, when using chlorine concentrations ranging from 6.5 and 13.6 mg/L and contact times up to 40 minutes.

### 3.6.2. Ozonation

Ozone is produced when oxygen molecules are dissociated by an energy source into oxygen atoms and subsequently collide with the non-dissociated oxygen molecules. Ozone is one of the most powerful oxidizing agents ( $E^0 = 2.07$  V) and it is mostly used to destroy organic compounds [215].

The oxidation of the target compounds can occur through two different mechanisms: i) direct reaction with molecular ozone or ii) indirect reaction with secondary oxidants formed upon the decomposition of ozone in water. Such decomposition is catalyzed by hydroxide ions (OH<sup>-</sup>) and other solutes. Highly reactive secondary oxidants, such as hydroxyl radicals (OH<sup>\*</sup>), are thereby formed. These radicals and their reaction products can cause the decomposition of ozone. Consequently, radical-type chain reactions may occur, which consume ozone concurrently with the direct reaction of ozone with dissolved organic material and contributing to the formation of additional hydroxyl radicals – Fig. 4 [216].

Ozone reacts with polysaccharides slowly, leading to breakage of glycosidic bonds and formation of aliphatic acids and aldehydes. The reaction of ozone with primary and secondary aliphatic alcohols may lead to formation of hydroxy-hydroperoxides, precursors to hydroxyl radicals, which in turn react strongly with the hydrocarbons [217]. However, it was already shown that N-acetyl glucosamine, a

compound present in the peptidoglycan of bacterial cell walls, was resistant to the action of ozone in aqueous solution at pH 3 to 7. This explains the higher resistance of Gram-positive bacteria compared to Gram negative ones, because the former contains higher amounts of peptidoglycan in their cell walls than the latter. Ozone can react significantly with amino acids and peptides, especially at neutral and basic pH. Furthermore, ozone reacts quickly with nucleobases, especially thymine, guanine, and uracil. Reaction of ozone with the nucleotides releases the carbohydrate and phosphate ions [217].

Ozone is mainly used for water treatment, however the use of ozone for surface disinfection was already reported [218]. Water disinfection by ozonation has been extensively reported, and some of the works are summarized in Table 5. Low ozone concentrations (0.15-0.20 mg/L) and contact time (180 s) were sufficient to inactivate several Gram negative bacteria in suspension to values up to 99.99% [219]. Nebel and co-workers [220] reported one of the first works describing the treatment of wastewater by ozonation. In this work, with an ozone dose of 14 mg/L and a contact time of 5 minutes it was possible to achieve log reduction values of up to 3 log for enterococci, total coliforms and fecal coliforms.

### 3.6.3. UV

Ultraviolet processing involves the use of radiation from the ultraviolet region of the electromagnetic spectrum for purposes of disinfection. Usually, the range of UV refers to wavelengths between 100 and

Table 5. Inactivation of several microorganisms by ozonation.

Domain	Phylum	Organism	Type of suspension	Type of Trial	Disinfection O <sub>3</sub> dose (mg/l)	Contact time (min)	Final Ozone Concentrations (mg/L)	Initial cellular density (CFU/mL)	Reduction (log)	Reference
Bacteria	Firmicutes	<i>Bacillus subtilis</i> spores	Axenic	Surface	16	150	n.a.	10 <sup>5</sup> -10 <sup>6</sup>	0.5	[218]
		<i>Enterococci</i>	Wastewater	Suspension	2-14	5-30	0.05-0.4	n.a.	1-3	[220-223]
		<i>Leuconostoc mesenteroides</i>	Axenic	Suspension	0.2 – 3.8	2	0	10 <sup>9</sup>	7	[224]
		<i>Listeria monocytogenes</i>	Axenic	Suspension	0.2 – 3.8	2	0	10 <sup>9</sup>	7	[224]
		<i>Staphylococcus aureus</i>	Axenic	Suspension	<sup>a</sup>	n.a.	2	10 <sup>7</sup>	7	[225]
		<i>Aeromonas salmonicida</i>	Axenic	Suspension	0.15-0.20	3	0.05-0.07	10 <sup>9</sup>	4	[219]
		<i>Escherichia coli</i>	Axenic	Surface	0.2 – 4	2-30	0.1-0.4	10 <sup>5</sup> -10 <sup>9</sup>	2-7	[218,221, 223-2236]
		<i>Fecal coliforms</i>	Wastewater	Suspension	7-14	5	0.05	n.a.	1-3	[220]
		<i>Pseudomonas fluorescens</i>	Wastewater	Suspension	0.2 – 3.8 <sup>a</sup>	2	2	10 <sup>9</sup>	7	[224,225]
		<i>Salmonella enterica</i>	Axenic	Suspension	<sup>a</sup>	n.a.	2	10 <sup>7</sup>	7	[225]
		<i>Shigella flexneri</i>	Axenic	Suspension	<sup>a</sup>	n.a.	2	10 <sup>7</sup>	7	[225]
		<i>Total coliforms</i>	Wastewater	Suspension	7-14	5	0.05	n.a.	2-3	[220,226]
		<i>Vibrio anguillarum</i>	Axenic	Suspension	0.15-0.20	3	0.05-0.07	10 <sup>9</sup>	4	[219]
		<i>Vibrio cholerae</i>	Axenic	Suspension	<sup>a</sup>	n.a.	2	10 <sup>7</sup>	7	[225]
		<i>Vibrio salmonicida</i>	Axenic	Suspension	0.15-0.20	3	0.05-0.07	10 <sup>9</sup>	4	[219]
		<i>Yersinia ruckeri</i>	Axenic	Suspension	0.15-0.20	3	0.05-0.07	10 <sup>9</sup>	4	[219]

		Total	Treated	Suspension	50 <sup>b</sup>	30	0	10 <sup>6</sup>	6	[223]
		heterotrophic bacteria	Wastewater							
<i>Eukarya</i>	<i>Apicomplexa</i>	<i>Cryptosporidium parvum</i>	Axenic	Suspension	0.36-2.2	1	n.a.	n.a.	6	[227]
	<i>Ascomycota</i>	<i>Aspergillus niger</i>	Wastewater	Suspension	50 <sup>b</sup>	30	0	10 <sup>3</sup>	3	[223]
		<i>Penicillium citrinum</i>	Axenic	Surface	16	120	n.a.	10 <sup>5</sup> -10 <sup>9</sup>	2	[218]
	<i>Basidiomycota</i>	<i>Rhodotorula rubra</i>	Wastewater	Suspension	50 <sup>b</sup>	30	0	10 <sup>3</sup>	3	[223]

a – Flow rate of 152.4 cm<sup>3</sup>/h, b - grams of ozone per normal cubic meter, n.a. – not available

400 nm. This range can be further subdivided. UVA corresponds to wavelengths between 315 and 400 nm and it is normally responsible for change in human skin that cause tanning; UVB refers to wavelengths between 280 and 315 nm and is the main responsible for skin burning and can also lead ultimately to skin cancer. UVC – 200 to 280 nm – is called the germicidal range, because it is considered to be the most effective towards the inactivation of bacteria and viruses. Finally, the vacuum UV range (100 to 200 nm), can be absorbed by almost all substance and can only be transmitted in the vacuum [228].

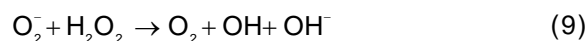
Among the above mentioned disinfection methods, UV light has been adopted as the most appropriate treatment process for drinking water because it is simple to use, highly effective for inactivating microbes and it does not introduce chemicals or cause the production of harmful disinfection by-products in the water [229]. This method promotes additional security after traditional treatment processes [230,231]. UV radiation is responsible for a wide range of biological effects [232-234], including modifications in the protein structure and in the DNA [235]. Regarding DNA damage, it may result on inhibition of cell replication and, in case of lethal doses, on the loss of ability to reproduce. Although the UV-A wavelengths bordering on visible light are not sufficiently energetic to directly modify DNA bases, cellular membrane damage can be induced through the production of ROS, such as singlet oxygen, superoxide, hydrogen peroxide and hydroxyl radical, generated via excitation of dissolved oxygen in water [177,236]. Furthermore, according to several authors, the damage induced by UV radiation continues even after the end of the irradiation period [236,237]. Bacterial DNA is a critical target of UV radiation and its effects depend on several parameters, such as UV spectrum, dissolved oxygen concentration, salt concentration and post-irradiation growth conditions [236]. Different microorganisms respond differently to the lethal effects of UV. It is known that the effectiveness of a UV disinfection system depends on the sensitivity of the target microorganisms to UV, microbial content, antibiotic resistance phenotypes, light source, UV radiation intensity, exposure time of microorganisms to radiation and their ability to re-growth [120,223,236-238]. UV treatment can be used for the inhibition of microorganisms in surfaces, in the air or in water [239-241].

Some works reporting the use of UV radiation on the inactivation of microorganisms are presented in Table 6. When using a light intensity of 2 W/m<sup>2</sup>, it

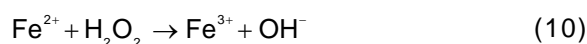
was possible to achieve high values of inactivation of different microorganisms in wastewater samples. A contact time of 50 seconds permitted to achieve log reductions of 4 to 5 for methicillin-resistant *Staphylococcus aureus* (MRSA), *E. coli*, and *Pseudomonas aeruginosa*. A higher contact time (100 s) was needed to reach similar log reduction values for vancomycin resistant *Enterococcus faecium* (VRE) [242]. In a study assessing the effectiveness of UV radiation on the inactivation of several vegetative bacteria (*Staphylococcus aureus*, *Enterococcus faecalis*, *E. coli*, *Salmonella enterica*, *Shigella sonnei*) *Bacillus subtilis* spores, *Acanthamoeba castellanii* cysts and viruses (poliovirus type 1 and simian rotavirus SA11), Chang and co-workers [243] reported that viruses, spores and cysts were 3-4, 9 and 15 times more resistant than the vegetative bacteria, respectively.

### 3.6.4. Hydrogen peroxide

Hydrogen peroxide is a metastable molecule – it easily decomposes into water and oxygen - with high redox potential (1.77 V) [244]. Even though the mechanism of hydrogen peroxide inactivation towards cells is usually attributed to the production of highly reactive hydroxyl radical, hydrogen peroxide itself presents some cytotoxicity towards cells. H<sub>2</sub>O<sub>2</sub> can directly oxidize the catalytic iron atom of dehydratase clusters, precipitating iron loss and enzyme inactivation. H<sub>2</sub>O<sub>2</sub> poisons the Isc system, which is responsible for the transfer of [4Fe-4S] clusters to newly synthesized apoenzymes. However, the mechanism of cytotoxic activity of H<sub>2</sub>O<sub>2</sub> is generally reported as based on the production of highly reactive hydroxyl radicals from the interaction of the superoxide (O<sub>2</sub><sup>•-</sup>) radical and H<sub>2</sub>O<sub>2</sub>, a reaction first proposed by Haber and Weiss [245] (Eq. (9)):



Further, it is believed that the production of extremely short-lived hydroxyl radicals within the cell by the Haber–Weiss cycle is catalyzed in vivo by the presence of transition metal ions (particularly iron-II) according to Fenton chemistry [246] (Eq. (10)):



The iron released from oxidized metalloproteins enlarges its intracellular pool, favoring the production of hydroxyl radical through the Fenton reaction [247]. The production of hydroxyl radical is, as described before, of utmost importance in the inactivation of microorganisms, accelerating the process of DNA damaging [217].

**Table 6.** Inactivation of several microorganisms with the use of UV radiation.

Domain	Phylum	Microorganism	Type of suspension	Type of trial	Irradiance (W/m <sup>2</sup> )	Contact time (min)	Initial cellular density (CFU/mL)	Log reduction	Reference		
Bacteria	Firmicutes	<i>Bacillus subtilis</i> spores	Axenic	Suspension	45 <sup>a</sup>	a	10 <sup>5</sup> -10 <sup>6</sup>	99.9 <sup>b</sup>	[243]		
		<i>Clostridium difficile</i> Spores	Axenic	Surface	36000 <sup>c</sup>	17	10 <sup>6</sup> -10 <sup>7</sup>	3	[241]		
		<i>Enterococci</i>	Wastewater	Suspension	e.g	180	10 <sup>5</sup>	2	[143,223]		
		Vancomycin-resistant	Wastewater	Suspension	12000 <sup>c</sup>	17(100 <sup>d</sup> )	10 <sup>5</sup> -10 <sup>7</sup>	5	[241,242]		
		<i>Enterococcus</i> (VRE)	Axenic	Surface							
		<i>Enterococcus faecalis</i>	Axenic	Suspension	80-100 (45 <sup>a</sup> )	10 (a)	10 <sup>5</sup> -10 <sup>7</sup>	1.2 (99.9 <sup>b</sup> )	[212,243]		
		<i>Staphylococcus aureus</i>	Axenic	Suspension	45 <sup>a</sup>	a	10 <sup>5</sup> -10 <sup>6</sup>	99.9 <sup>b</sup>	[243]		
		Methicillin-resistant	Wastewater	Suspension	12000 <sup>c</sup>	17(50 <sup>d</sup> )	10 <sup>5</sup> -10 <sup>7</sup>	4	[241,242]		
		<i>Staphylococcus aureus</i> (MRSA)	Axenic	Surface							
		<i>Acinetobacter baumannii</i>	Axenic	Surface	12000 <sup>c</sup>	17	10 <sup>6</sup> -10 <sup>7</sup>	4	[241]		
		<i>Escherichia coli</i>	Wastewater Axenic	Suspension	100-140 <sup>g</sup>	10-120(50 <sup>d</sup> )	10 <sup>5</sup> -10 <sup>7</sup>	5	[120,212,223,242,243]		
		Proteobacteria		<i>Pseudomonas aeruginosa</i>	Wastewater Axenic	Suspension	f	120(50 <sup>d</sup> )	10 <sup>7</sup>	5	[120,242]
				<i>Salmonella enterica</i>	Axenic	Suspension	f	120	10 <sup>7</sup>	3	[120,243]
				<i>Salmonella enteritidis</i>	Axenic	Suspension	60-100	10	10 <sup>5</sup> -10 <sup>7</sup>	3	[212]
<i>Shigella sonnei</i>	Axenic			Suspension	45 <sup>a</sup>	a	10 <sup>5</sup> -10 <sup>6</sup>	99.9 <sup>b</sup>	[243]		
Total Coliforms	Wastewater Axenic			Suspension	1.5-45 <sup>a</sup> (e)	2, a	10 <sup>5</sup> -10 <sup>6</sup>	3 (99.9 <sup>b</sup> )	[143,180,243]		
<i>Vibrio anguillarum</i>	Axenic			Suspension	30	n.a.	10 <sup>7</sup>	5	[219]		
<i>Vibrio salmonicida</i>	Axenic			Suspension	30	n.a.	10 <sup>7</sup>	5	[219]		
<i>Yersinia ruckeri</i>	Axenic	Suspension	30	n.a.	10 <sup>7</sup>	5	[219]				

-	Total heterotrophic bacteria	Wastewater	Suspension	<sup>g</sup>	30	10 <sup>6</sup>	6	[223]		
<i>Eukarya</i>	<i>Acanthamoeba castellanii</i> cysts	Axenic	Suspension	45 <sup>a</sup>	a	10 <sup>5</sup> -10 <sup>6</sup>	99.9 <sup>b</sup>	[243]		
	Ascomycota	Wastewater	Suspension	<sup>g</sup>	30	10 <sup>3</sup>	3	[223]		
	Basidiomycota	Wastewater	Suspension	<sup>g</sup>	30	10 <sup>3</sup>	3	[223]		

a- UV dose – mW.s/cm<sup>2</sup>, b- %, c- mWs/cm<sup>2</sup>, d – seconds, e - 800 W UV-lamp, f –3.42 × 10<sup>-5</sup> Einsteins s<sup>-1</sup>, g - low-pressure mercury lamp (emission line at 254 nm), n.a. – not available.

$H_2O_2$  can be used in both liquid and vapor phases. Hence, it is used in water disinfection (liquid phase) or in the disinfection of surfaces (vapor phase). Indeed, it is believed that the vapor phase has higher kinetic energies and is uncharged, so it can surround and penetrate the three-dimensional protein structures more easily, oxidizing buried cysteine residues and breaking vulnerable bonds between subunits [248]. Thus, an enhanced antimicrobial activity of hydrogen peroxide vapor when compared to its liquid state is usually reported [249-252].

Some studies reporting the utilization of hydrogen peroxide as a disinfectant are summarized in Table 7. Otter and co-workers [251] studied the effectiveness of hydrogen peroxide on the inactivation of nosocomial bacteria and spores on surfaces. After 90 minutes of contact with hydrogen peroxide vapor, all of the tested microorganisms were completely inactivated (Log reduction of 6). However, differences on the resistance against the hydrogen peroxide vapor treatment were observed. *Acinetobacter* showed the highest resistance to this treatment, while vancomycin-resistant enterococci were the first to be completely inactivated, after only 10 minutes of treatment. Hydrogen peroxide is also suitable to disinfect wastewater. Indeed, the density of total coliforms in wastewater was reduced 4 fold when using  $H_2O_2$  up to 2.5 mL/L and a contact time of 3 h [253].

### 3.7. Comparison between photoinactivation and traditional disinfection methods

In contrast with the traditional disinfection methods described above,  $TiO_2$ -UV photocatalysis is not yet considered as an established water disinfection technology [255]. However, until this date, several reports showed the potential of this technique for disinfecting. Indeed, photocatalysis is a versatile and effective process that can be adapted for use in many applications for disinfection in both air and water matrices. Additionally, improved photocatalytic coatings are being developed, tested and even commercialized for use in the context of "self-disinfecting" materials. In this sense, the strength of photocatalytic disinfection lies in its versatility for use in many different applications [256]. Indeed, photocatalytic-based products already reached a global volume of US\$848 Million in 2009 of which over 87% were related to products with self-cleaning activity used for construction [257]. Among these are glass coatings, cements and textile fibers [257],

commercialized by companies such as Pilkington, Italcementi Group and Taiheiyou Cement. Coatings and ceramics with antimicrobial activity are also commercialized by several companies. Deutsche Steinzeug company, which commercializes flags, tiles and sanitary ceramics and, company Kurare, which commercializes textile fibers containing  $TiO_2$  photocatalysts, should be highlighted. Japanese Arc-Flash, the first company commercializing photocatalyst-based materials in 1992, uses a photocatalyst fixation technology that allows spraying the photocatalytic product directly on surfaces. The photocatalytic coating produced by Arc-Flash uses titania nanoparticles as main ingredient and is used to sterilize mildew, sanitize environments such as hospitals, residential kitchens, schools, and floors, killing bacteria with over 98% efficiency [257].

The versatility mentioned for photocatalysis is also reported for UV radiation. Advances in the optimization of UV reactors permitted to inactivate a high variety of waterborne microorganisms in few seconds [242]. However, there are still some limitations on the use of this technique. Very high values of irradiation (in most cases over 50 W/m<sup>2</sup>) must be used to inactivate some microorganisms (Table 6), and even under these harsh conditions, inactivation of some microbial forms, such as *Clostridium difficile* spores, is not possible. Several studies where the effectiveness of UV treatment was directly compared with photocatalysis demonstrated that, as expected, UV treatment was less efficient than  $TiO_2$ -UV [105,116,118]. The use of a photocatalyst, in most cases decreases the need of high irradiation intensity and promotes the decrease of contact times. Ibanez and co-workers [116] verified that it was not possible to inactivate *Enterobacter cloacae*, *E. coli*, *P. aeruginosa* and *Salmonella typhimurium* with an UV irradiance of 55 W/m<sup>2</sup>. However, when coupling UV irradiation with 0.1 g/L  $TiO_2$ , log reduction values around 6 were achieved for all the tested strains for the same time of contact. The decrease of contact time from 360 to 50 minutes to achieve 3 log reduction of the total heterotrophic bacteria of wastewater was also reported [118], when using a photon flux of approximately 390 mmol/h and 5 g/L of photocatalyst. More recently, Lin and co-workers [180] showed that it was possible to reduce the load of the total coliforms in wastewater 4 fold, when irradiance of 1.5 W/m<sup>2</sup> and a contact time of 120 s was coupled with the presence of a  $TiO_2$  coated reactor, while a 3 fold reduction was obtained in the absence of the photocatalyst.

Ozonation is a technique that can promote total inactivation of most types of microorganisms under

**Table 7.** Inactivation of several microorganisms with the use hydrogen peroxide.

Domain	Phylum	Organism	Type of suspension	Type of trial	Hydrogen peroxide concentration (mL/L)	Contact time(min)	Initial cellular density (CFU/mL)	Log reduction	Reference
Bacteria	Firmicutes	<i>Bacillus subtilis</i>	Axenic	Surface	a	32	10 <sup>6</sup>	100 <sup>b</sup>	[252]
		<i>Enterococcus faecalis</i>	Axenic	Suspension	3-150	10	10 <sup>5</sup> -10 <sup>7</sup>	0.1	[212]
		<i>Enterococcus faecium</i>	Axenic	Surface	a	90	10 <sup>6</sup>	6	[251]
		<i>Geobacillus stearothermophilus</i>	Axenic	Surface	a	32-50	10 <sup>4</sup> -10 <sup>6</sup>	4 (100 <sup>b</sup> )	[252,254]
		<i>Staphylococcus aureus</i> (MRSA)	Axenic	Surface	a	50-90	10 <sup>4</sup> -10 <sup>6</sup>	6	[251,254]
		Vancomycin-resistant <i>Enterococcus</i> (VRE)	Axenic	Surface	a	50 - 90	10 <sup>4</sup> - 10 <sup>6</sup>	6	[251,254]
		<i>Clostridium difficile</i>	Axenic	Surface	a	50 - 90	10 <sup>4</sup> - 10 <sup>6</sup>	6	[251,254]
		<i>Acinetobacter baumannii</i>	Axenic	Surface	a	90	10 <sup>6</sup>	6	[251]
		<i>Acinetobacter</i> sp.	Axenic	Surface	a	90	10 <sup>6</sup>	6	[251]
		Fecal Coliforms	Wastewater	Suspension	2.5	240	10 <sup>6</sup>	4	[253]
		<i>Klebsiella pneumoniae</i>	Axenic	Surface	a	90	10 <sup>6</sup>	6	[251]

a- Hydrogen Peroxide Vapor (HPV) was used, b -%.

low contact times, in most cases under 20 minutes, and with low  $O_3$  doses, at most 4 mg/L – Table 5. However, it is important to note that ozonation may cause the formation of very harmful by products, specially bromide and other brominated compounds [258]. Rizzo and co-workers [259] compared the efficiency of ozonation and photocatalysis for the treatment of urban wastewaters. In this work, it was shown that it was possible to obtain increased degradation of organic matter with the photocatalytic oxidation process, even at low  $TiO_2$  concentrations. Furthermore, a 30 min photocatalytic treatment was found to produce an effluent complying with the trihalomethanes limit set by Italian regulation for wastewater reuse. Furthermore, the cost associated to the use of ozonation is still very high [260]. Additionally, the coupling of ozonation with photocatalysis was already studied. Moreira and co-workers [261] reported the use of photocatalytic ozonation for the disinfection of urban treated wastewaters. In this study, a photocatalytic ozonation system using  $TiO_2$ -coated glass Raschig rings with LEDs irradiation - two 10 W UV high intensity LEDs with dominant emission line at 382 nm - was tested in continuous mode. This study reported the reduction of enterococci, enterobacteria, and fungi from  $10^5$  -  $10^6$  CFU/100 mL to values around or below  $10^1$  CFU/100 mL; total heterotrophs presented lower reductions, but still reaching values of around  $10^2$  CFU/100 mL after the treatment.

The use of hydrogen peroxide to disinfect water requires, usually, high contact times (up to 240 minutes) or concentrations (up 150 mL/L) (Table 7). Lower contact times (90 minutes) are required to inactivate the microorganisms when the vapor phase is used (Table 7), suggesting that hydrogen peroxide is a good technique to disinfect surfaces. However, the toxic effects of  $H_2O_2$ , require the interdiction of the site to be disinfected [262] for periods up to 1 hour and 40 minutes. Also chlorination requires high contact times (up to 120 minutes) to be effective on the inactivation of microorganisms (Table 4). Additionally, some microorganisms are resistant to chlorination treatments [263,264]. Nevertheless, it is important to note that nowadays chlorination remains as the most used disinfection method [265]. This is mainly due to the fact that the new alternative processes require expensive chemicals or costly equipment to generate the disinfectant onsite. However, chlorination causes the formation of several highly toxic by-products. Among these, it is important to highlight the formation of trihalomethanes and dichloroacetic acid that are believed to be carcinogenic [266]. The existence of

these dangerous by-products leads to the necessity of coming up with suitable alternatives to chlorination. The main advantages and disadvantages of each of these techniques are summarized in Table 8.

Although promising, photocatalysis still faces some drawbacks when imposing itself as a reference disinfection technique. As for other disinfection methods, re-growth after photocatalytic treatment may occur [223,261]. In addition, one of the main problems, usually disregarded by most of works conducted up to now in this field, is the absence of knowledge on the long time effect of photoinactivation. Little is known on the type of organisms able to tolerate the oxidative stress imposed by photocatalysis; however, increased tolerance of antibiotic resistant bacteria when compared with the susceptible counterpart is reported [106]. This observation points out for the need of further studies on the type and fate of the organisms surviving the treatment. This is particularly important, because under real conditions it may be not economically feasible to use conditions guaranteeing the inactivation without regrowth of potentially dangerous microorganisms [267]. Furthermore, and in order to be applied in full scale, the optimization of the photocatalyst to fully take advantage of the visible light spectrum should be achieved. This optimization should be focused in the future either by the optimization of the photocatalytic material ( $TiO_2$ ) or by the use of suitable supports (for example graphene).

Although being a very promising disinfection technology, the massive use of  $TiO_2$  nanoparticles without a proper evaluation concerning of their antimicrobial potential can produce negative drawbacks. Indeed, using  $TiO_2$  nanoparticles, even in those products not directly designed for disinfection, may cause the propagation of the aforementioned antibiotic and oxidative stress resistant microorganism in a worrisome scale. Thus, the definition of new standards to test the efficacy of photocatalytic systems, including organisms with high tolerance to oxidative stress and antibiotics, is a subject of utmost importance in nowadays society.

#### 4. CONCLUSIONS

$TiO_2$ -anatase is presently the most used photocatalyst for environmental applications due to its high stability, good location of the band edges, low charge transport resistance, high photocatalytic activity, high chemical and thermal stability, low toxicity and low price. However, to increase the usefulness of

**Table 8.** Comparison between the different disinfection techniques.

Disinfection Technique	Chlorination	Ozonation	Ultraviolet radiation	Hydrogen Peroxide	Photocatalysis
Advantages	<ul style="list-style-type: none"> <li>• Inexpensive;</li> <li>• Relatively easy to handle, simple to dose, measure and control;</li> <li>• Proven to be effective against a wide variety of bacteria and viruses;</li> </ul>	<ul style="list-style-type: none"> <li>• One of the most effective disinfectants; widely used to inactivate pathogens in drinking water;</li> <li>• Needs short contact times;</li> <li>• Generated onsite, leading to fewer safety issues than other techniques;</li> </ul>	<ul style="list-style-type: none"> <li>• Simple to use</li> <li>• Highly effective for inactivating microorganisms;</li> <li>• Does not introduce chemicals or cause the production of harmful disinfection by-products in the water;</li> <li>• High versatility – can be applied to wastewater, air and surfaces treatment;</li> </ul>	<ul style="list-style-type: none"> <li>• Considered environmentally friendly because it can rapidly degrade into the innocuous products water and oxygen;</li> <li>• Demonstrates broad-spectrum efficacy against viruses, bacteria, yeasts, and bacterial spores</li> </ul>	<ul style="list-style-type: none"> <li>• Capable of inactivating microorganisms, including viruses, bacteria, spores and protozoa;</li> <li>• Does not cause the production of harmful disinfection by-products in water;</li> <li>• <math>\text{TiO}_2</math> is cheap, innocuous and can be attached to different types of inert matrices;</li> <li>• Useful in developing countries where electricity is not available;</li> <li>• High versatility – can be applied to disinfect water, air and surfaces;</li> <li>• Uses nanoparticles than can be harmful for the general health;</li> <li>• Its mainly active in the UV range, presenting still some limitations using visible light;</li> <li>• When used in suspension, brings complexity to the process for the recuperation of the photocatalyst;</li> </ul>
Disadvantages	<ul style="list-style-type: none"> <li>• Some organisms tend to develop resistance and require a concentration higher than normal, diminishing the quality of water;</li> <li>• Formation of hazardous disinfection by-products, specially trihalomethanes (THMs) and nitrosamines;</li> <li>• Residuals are highly toxic to aquatic life; hence, a dechlorination step is needed;</li> </ul>	<ul style="list-style-type: none"> <li>• Formation of potentially harmful byproducts including bromate and other brominated disinfection by-products;</li> <li>• Due to its instability, ozone must be generated before use, which leads to high equipment and operating costs;</li> <li>• Low dosage may not effectively inactivate some viruses, spores and cysts;</li> </ul>	<ul style="list-style-type: none"> <li>• Needs shortwave radiation (&lt;280 nm), which requires the set up of expensive lighting equipment and is associated with increased energy utilization;</li> <li>• Organisms can sometimes repair and reverse the destructive effects of UV (photo-activation);</li> <li>• The presence of solid particles in water can affect severely the UV efficiency;</li> </ul>	<ul style="list-style-type: none"> <li>• The presence of catalase or other peroxidases in these organisms can increase tolerance, when conjugated with lower concentrations of <math>\text{H}_2\text{O}_2</math>;</li> <li>• Higher concentrations of <math>\text{H}_2\text{O}_2</math>, between 10 and 30 %, and longer contact times are required for inactivation of spores;</li> <li>• During the <math>\text{H}_2\text{O}_2</math> treatment the sites where</li> </ul>	<ul style="list-style-type: none"> <li>• The presence of catalase or other peroxidases in these organisms can increase tolerance, when conjugated with lower concentrations of <math>\text{H}_2\text{O}_2</math>;</li> <li>• Higher concentrations of <math>\text{H}_2\text{O}_2</math>, between 10 and 30 %, and longer contact times are required for inactivation of spores;</li> <li>• During the <math>\text{H}_2\text{O}_2</math> treatment the sites where</li> </ul>

- Mainly applied and limited to water treatment and surface cleaning;
- Lacks long residual activity, limiting its application in large distribution systems;
- Mainly limited to water treatment, but can be used also for surface disinfection;
- Low dosage may not effectively inactivate some viruses, spores, and cysts;
- During the UV treatments the sites where the treatments are applied are interdicted to humans due to the harmful effect of this type of radiation;
- The treatments are applied and are interdicted to humans due to the harmful effect of this chemical compound;

References [207,268]

[269-271]

[229,232-234,272]

[247,273]

[265,274,275]

titanium dioxide, it is necessary to increase its photoactivity and ability to absorb visible light. This review article presents an overview of the fundamentals of photocatalysis and briefly reviews the most relevant strategies to enhance the photocatalytic activity of TiO<sub>2</sub>, aiming ultimately the indoor photoinactivation of harmful biological agents. Since TiO<sub>2</sub> may contribute to prevent nosocomial infections, its practical application in this field is strongly envisaged. TiO<sub>2</sub> photocatalysis, similarly to the phagocytic cells of the human immune system, use the cytotoxic effects of Reactive Oxygen Species (ROS) to inactivate microorganisms. These ROS are known to be highly reactive with biological molecules and thus they are effective for the inactivation various different types of microorganisms.

Photoinactivation of microorganisms under UV radiation using TiO<sub>2</sub> has been thoroughly studied with great success; a wide diversity of microorganisms has been studied, Gram-negative and Gram-positive bacteria, including dormant forms (cysts, spores) fungi, algae and protozoa. Targeting future commercial applications, the research was directed to the use of visible light instead of only on UV radiation, and of proper immobilization of the photocatalyst. TiO<sub>2</sub> doping and/or decoration with the objective of increasing photoactivity and photoabsorbance were briefly reviewed as well as the use of TiO<sub>2</sub>/graphene composite photocatalysts. The use of graphene reduces the risks of health hazards because in TiO<sub>2</sub>/graphene composites TiO<sub>2</sub> nanoparticles are attached to micro-size graphene platelets that prevent the catalyst to be absorbed by the human body. In the case of TiO<sub>2</sub>/graphene composite photocatalyst, the decoration of TiO<sub>2</sub> with metals such as Ag and Au further decrease charge recombination, show plasmonic effect and reduce the redox overpotentials.

Although promising, photocatalysis still faces some drawbacks when imposing itself as a reference disinfection technique. Besides the mentioned limitations regarding the optimization of photocatalysts to attain visible light activity, the absence of knowledge on the long time effect of photoinactivation on microorganisms should be a matter of concern.

## ACKNOWLEDGEMENTS

Pedro Magalhães is grateful to the Portuguese Foundation for Science and Technology (FCT) for his PhD Grant (Reference: SFRH/BD/78827/2011). Luísa Andrade acknowledges European Research Council for funding within project BI-DSC (contract ERC

n 321315). This work was financially supported by the projects POCl-01-0145-FEDER-006939 - Laboratory for Process Engineering, Environment, Biotechnology and Energy – LEPABE and NORTE 01 0145 FEDER 000005 – LEPABE-2-ECO-INNOVATION, funded by FEDER funds through COMPETE2020 - Programa Operacional Competitividade e Internacionalização (POCl) and Programa Operacional Regional do Norte (NORTE2020) and by national funds through FCT - FundaçãPo para a Ciencia e a Tecnologia and was also partially funded by the project “Synthesis and characterization of new TiO<sub>2</sub>-graphene composite photocatalysts: application to NO<sub>x</sub> photoabatement and water splitting for hydrogen production.” (Reference: PTDC/EQU-EQU/115614/2009).

## REFERENCES

- [1] M. Ni, M.K.H. Leung, D.Y.C. Leung and K. Sumathy // *Renew. Sust. Energ. Rev.* **11** (2007) 401.
- [2] S. Banerjee, D.D. Dionysiou and S.C. Pillai // *Appl. Catal. B-Environ.* **176–177** (2015) 396.
- [3] F. Kapteijn, J. Rodriguez-Mirasol and J.A. Moulijn // *Appl. Catal. B-Environ* **9** (1996) 25.
- [4] M. Kaneko and I. Okura, In: *Photocatalysis: Science and Technology* (Kodansha, 2002), p. 123.
- [5] J.H. Carey, J. Lawrence and H.M. Tosine // *Bull. Environ. Contam. Toxicol.* **16** (1976) 697.
- [6] M. Kaneko and I. Okura, In: *Photocatalysis: Science and Technology* (Kodansha, 2002), p. 157.
- [7] T. Matsunaga, R. Tomoda, T. Nakajima and H. Wake // *FEMS Microbiol. Lett.* **29** (1985) 211.
- [8] B. Meyer and B. Cookson // *J. Hosp. Infect.* **76** (2010) 200.
- [9] B. Spellberg, R. Guidos, D. Gilbert, J. Bradley, H.W. Boucher, W.M. Scheld, J.G. Bartlett and J. Edwards // *Clin. Infect. Dis.* **46** (2008) 155.
- [10] World Health Organization, *The world health report 2007 - A safer future: global public health security in the 21st century* (World Health Organization, Geneva, Switzerland, 2007).
- [11] H.A. Foster, I.B. Ditta, S. Varghese and A. Steele // *Appl. Microbiol. Biotechnol.* **90** (2011) 1847.
- [12] A. Fujishima and K. Honda // *Nature* **238** (1972) 37.
- [13] A. Di Paola, M. Bellardita and L. Palmisano // *Catalysts* **3** (2013) 36.

- [14] T.A. Kandiel, L. Robben, A. Alkaim and D. Bahnemann // *Photoch. Photob. Sci.* **12** (2013) 602.
- [15] D.C. Hurum, A.G. Agrios, K.A. Gray, T. Rajh and M.C. Thurnauer // *J. of Phys. Chem. B* **107** (2003) 4545.
- [16] T. Kawahara, Y. Konishi, H. Tada, N. Tohge, J. Nishii and S. Ito // *Angew. Chem.* **114** (2002) 2935.
- [17] A. Mills, C. O'Rourke and K. Moore // *J. Photoch. Photobio. A* **310** (2015) 66.
- [18] B. Liu, X. Zhao, C. Terashima, A. Fujishima and K. Nakata // *PCCP* **16** (2014) 8751.
- [19] C.S. Turchi and D.F. Ollis // *J. Catal.* **122** (1990) 178.
- [20] J. Ângelo, *Development and Characterization of Titania-based Photocatalysts and their Incorporation in Paint Coatings* (Chemical Engineering Department, Faculty of Engineering of the University of Porto, Porto, 2016).
- [21] P. Salvador // *J. of Phys. Chem. C* **111** (2007) 17038.
- [22] J.F. Montoya, M.F. Atitar, D.W. Bahnemann, J. Peral and P. Salvador // *J. of Phys. Chem. C* **118** (2014) 14276.
- [23] R.A. Marcus // *J. Chem. Phys.* **24** (1956) 966.
- [24] J.F. Montoya, J. Peral and P. Salvador // *J. of Phys. Chem. C* **118** (2014) 14266.
- [25] R. Dillert, A. Engel, Gro, P. Lindner and D.W. Bahnemann // *PCCP* **15** (2013) 20876.
- [26] A. Zaleska // *Recent Patents on Engineering* **2** (2008) 157.
- [27] B. Ohtani, Y. Ogawa and S.I. Nishimoto // *J. Phys. Chem. B* **101** (1997) 3746.
- [28] B. Ohtani, K. Iwai, S.I. Nishimoto and S. Sato // *J. Phys. Chem. B* **101** (1997) 3349.
- [29] N. Wu, J. Wang, D.N. Tafen, H. Wang, J.G. Zheng, J.P. Lewis, X. Liu, S.S. Leonard and A. Manivannan // *JACS* **132** (2010) 6679.
- [30] S. Rehman, R. Ullah, A.M. Butt and N.D. Gohar // *J. Hazard. Mater.* **170** (2009) 560.
- [31] R. Van De Krol and M. Grätzel, In: *Photoelectrochemical Hydrogen Production* (Springer, 2011), p. 13.
- [32] J. Blanco-Galvez, P. Fernandez-Ibanez and S. Malato-Rodriguez // *J. Sol. Energy Eng.* **129** (2007) 4.
- [33] G. Fu, P.S. Vary and C.-T. Lin // *J. of Phys. Chem. B* **109** (2005) 8889.
- [34] A. Ghicov, B. Schmidt, J. Kunze and P. Schmuki // *Chem. Phys. Lett.* **433** (2007) 323.
- [35] J.-M. Herrmann, J. Disdier and P. Pichat // *Chem. Phys. Lett.* **108** (1984) 618.
- [36] S.T. Martin, C.L. Morrison and M.R. Hoffmann // *J. Phys. Chem.* **98** (1994) 13695.
- [37] J. Moser, M. Grätzel and R. Gallay // *Helv. Chim. Acta* **70** (1987) 1596.
- [38] K. Wilke and H.D. Breuer // *J. Photoch. Photobio. A* **121** (1999) 49.
- [39] J.C.S. Wu and C.-H. Chen // *J. Photoch. Photobio. A* **163** (2004) 509.
- [40] J. Choi, H. Park and M.R. Hoffmann // *J. of Phys. Chem. C* **114** (2009) 783.
- [41] S.N.R. Inturi, T. Boningari, M. Suidan and P.G. Smirniotis // *Appl. Catal. B-Environ.* **144** (2014) 333.
- [42] R. Asahi, T. Morikawa, T. Ohwaki, K. Aoki and Y. Taga // *Science* **293** (2001) 269.
- [43] D. Chen, Z. Jiang, J. Geng, Q. Wang and D. Yang // *Ind. Eng. Chem. Res.* **46** (2007) 2741.
- [44] T. Lindgren, J.M. Mwabora, E. Avendaño, J. Jonsson, A. Hoel, C.-G. Granqvist and S.-E. Lindquist // *J. of Phys. Chem. B* **107** (2003) 5709.
- [45] R. Nakamura, T. Tanaka and Y. Nakato // *J. of Phys. Chem. B* **108** (2004) 10617.
- [46] W. Zhu, X. Qiu, V. Iancu, X.Q. Chen, H. Pan, W. Wang, N.M. Dimitrijevic, T. Rajh, H.M. Meyer, M.P. Paranthaman, G.M. Stocks, H.H. Weitering, B. Gu, G. Eres and Z. Zhang // *Phys. Rev. Lett.* **103** (2009) 226401.
- [47] C. Burda, Y. Lou, X. Chen, A.C.S. Samia, J. Stout and J.L. Gole // *Nano Lett.* **3** (2003) 1049.
- [48] T. Tachikawa, S. Tojo, K. Kawai, M. Endo, M. Fujitsuka, T. Ohno, K. Nishijima, Z. Miyamoto and T. Majima // *J. Phys. Chem. B* **108** (2004) 19299.
- [49] J. Xu, Y. Ao, D. Fu and C. Yuan // *Appl. Surf. Sci.* **254** (2008) 3033.
- [50] J.G. Yu, J.C. Yu, B. Cheng, S.K. Hark and K. lu // *J. Solid State Chem.* **174** (2003) 372.
- [51] H. Barndök, D. Hermosilla, C. Han, D.D. Dionysiou, C. Negro and Á. Blanco // *Appl. Catal. B-Environ* **180** (2016) 44.
- [52] N. Serpone // *J. of Phys. Chem. B* **110** (2006) 24287.
- [53] M. Pelaez, N.T. Nolan, S.C. Pillai, M.K. Seery, P. Falaras, A.G. Kontos, P.S.M. Dunlop, J.W.J. Hamilton, J.A. Byrne, K. O'Shea, M.H. Entezari and D.D. Dionysiou // *Appl. Catal. B-Environ* **125** (2012) 331.

- [54] S. Banerjee, S.C. Pillai, P. Falaras, K.E. O'Shea, J.A. Byrne and D.D. Dionysiou // *J. Phys. Chem. Lett.* **5** (2014) 2543.
- [55] X. Li, P. Liu, Y. Mao, M. Xing and J. Zhang // *Appl. Catal. B-Environ* **164** (2015) 352.
- [56] C. Di Valentin, G. Pacchioni, A. Selloni, S. Livraghi and E. Giamello // *J. Phys. Chem. B* **109** (2005) 11414.
- [57] W. Ren, Z. Ai, F. Jia, L. Zhang, X. Fan and Z. Zou // *Appl. Catal. B-Environ* **69** (2007) 138.
- [58] X. Ma, Y. Dai, M. Guo and B. Huang // *J. Phys. Chem. C* **117** (2013) 24496.
- [59] J.A. Rengifo-Herrera and C. Pulgarin // *Sol. Energy* **84** (2010) 37.
- [60] J.A. Rengifo-Herrera, K. Pierzchała, A. Sienkiewicz, L. Forró, J. Kiwi and C. Pulgarin // *Appl. Catal. B-Environ* **88** (2009) 398.
- [61] S.T. Kochuveedu, D.-P. Kim and D.H. Kim // *J. Phys. Chem. C* **116** (2011) 2500.
- [62] X. He, Y. Cai, H. Zhang and C. Liang // *J. Mater. Chem.* **21** (2011) 475.
- [63] H. Tran, J. Scott, K. Chiang and R. Amal // *J. Photoch. Photobio. A* **183** (2006) 41.
- [64] I.M. Arabatzis, T. Stergiopoulos, M.C. Bernard, D. Labou, S.G. Neophytides and P. Falaras // *Appl. Catal. B-Environ* **42** (2003) 187.
- [65] L.G. Devi and R. Kavitha // *Appl. Catal. B-Environ* **140–141** (2013) 559.
- [66] H. Park, Y. Park, W. Kim and W. Choi // *J. Photoch. Photobio. C* **15** (2013) 1.
- [67] S.G. Kumar and L.G. Devi // *J. Phys. Chem. A* **115** (2011) 13211.
- [68] R. Daghrir, P. Drogui and D. Robert // *Ind. Eng. Chem. Res.* **52** (2013) 3581.
- [69] Y. Wen, H. Ding and Y. Shan // *Nanoscale* **3** (2011) 4411.
- [70] S.S. Rayalu, D. Jose, M.V. Joshi, P.A. Mangrulkar, K. Shrestha and K. Klabunde // *Appl. Catal. B-Environ* **142–143** (2013) 684.
- [71] S. Bouhadoun, C. Guillard, F. Dapozze, S. Singh, D. Amans, J. Bouclé and N. Herlin-Boime // *Appl. Catal. B-Environ* **174–175** (2015) 367.
- [72] T. Hirakawa and P.V. Kamat // *JACS* **127** (2005) 3928.
- [73] A. Kudo and Y. Miseki // *Chem. Soc. Rev.* **38** (2009) 253.
- [74] K. Maeda, K. Teramura, D. Lu, N. Saito, Y. Inoue and K. Domen // *Angew. Chem.* **118** (2006) 7970.
- [75] J. Sato, H. Kobayashi, K. Ikarashi, N. Saito, H. Nishiyama and Y. Inoue // *J. Phys. Chem. B* **108** (2004) 4369.
- [76] G. Hu and B. Tang // *Mater. Chem. Phys.* **138** (2013) 608.
- [77] K. Zhou, Y. Zhu, X. Yang, X. Jiang and C. Li // *New J. Chem.* **35** (2011) 353.
- [78] S. Liu, H. Sun, S. Liu and S. Wang // *Chem. Eng. J.* **214** (2013) 298.
- [79] H. Zhang, X. Lv, Y. Li, Y. Wang and J. Li // *ACS Nano* **4** (2010) 380.
- [80] S. Malato, J. Blanco, A. Vidal and C. Richter // *Appl. Catal. B-Environ* **37** (2002) 1.
- [81] J. Petlicki and T.G.M. van de Ven // *J. Chem. Soc., Faraday Trans.* **94** (1998) 2763.
- [82] J.S. Lee, K.H. You and C.B. Park // *Adv. Mater.* **24** (2012) 1084.
- [83] G. Li, T. Wang, Y. Zhu, S. Zhang, C. Mao, J. Wu, B. Jin and Y. Tian // *Appl. Surf. Sci.* **257** (2011) 6568.
- [84] T.-D. Nguyen-Phan, V.H. Pham, E.W. Shin, H.-D. Pham, S. Kim, J.S. Chung, E.J. Kim and S.H. Hur // *Chem. Eng. J.* **170** (2011) 226.
- [85] A. Tanaka, S. Sakaguchi, K. Hashimoto and H. Kominami // *ACS Catalysis* **3** (2012) 79.
- [86] Y. Wang, J. Yu, W. Xiao and Q. Li // *J. Mater. Chem. A* **2** (2014) 3847.
- [87] V. Subramanian, E.E. Wolf and P.V. Kamat // *JACS* **126** (2004) 4943.
- [88] I. Vaz-Moreira, O.C. Nunes and C.M. Manaia // *FEMS Microbiology Reviews* **38** (2014) 761.
- [89] C. Baker-Austin, M.S. Wright, R. Stepanauskas and J.V. McArthur // *Trends Microbiol* **14** (2006) 176.
- [90] A. Hernandez, R.P. Mellado and J.L. Martinez // *Appl. Environ. Microbiol.* **64** (1998) 4317.
- [91] E. Miyahara, M. Nishie, S. Takumi, H. Miyanojima, J. Nishi, K. Yoshiie, H. Oda, M. Takeuchi, M. Komatsu, K. Aoyama, M. Horiuchi and T. Takeuchi // *FEMS Microbiol. Lett.* **317** (2011) 109.
- [92] A.C. Fluit and F.J. Schmitz // *Clin. Microbiol. Infect.* **10** (2004) 272.
- [93] B.M. Babior // *Am. J. Med.* **109** (2000) 33.
- [94] R.A. Miller and B.E. Britigan // *Clin. Microbiol. Rev.* **10** (1997) 1.
- [95] W.D. Splettstoesser and P. Schuff-Werner // *Microsc. Res. Tech.* **57** (2002) 441.
- [96] R.A. Clark // *J. Infect. Dis.* **161** (1990) 1140.
- [97] J.C. Ireland, P. Klostermann, E.W. Rice and R.M. Clark // *Appl. Environ. Microbiol.* **59** (1993) 1668.

- [98] Y. Kikuchi, K. Sunada, T. Iyoda, K. Hashimoto and A. Fujishima // *J. Photochem. Photobio. A* **106** (1997) 51.
- [99] P.C. Maness, S. Smolinski, D.M. Blake, Z. Huang, E.J. Wolfrum and W.A. Jacoby // *Appl. Environ. Microbiol.* **65** (1999) 4094.
- [100] M. Cho, H. Chung, W. Choi and J. Yoon // *Water Res.* **38** (2004) 1069.
- [101] I. Paspaltsis, K. Kotta, R. Lagoudaki, N. Grigoriadis, I. Poullos and T. Sklaviadis // *J. Gen. Virol.* **87** (2006) 3125.
- [102] V. Ramamurthy, *Organic Photochemistry* (Taylor & Francis, 1997).
- [103] J.-J. Huang, H.-Y. Hu, Y.-H. Wu, B. Wei and Y. Lu // *Chemosphere* **90** (2013) 2247.
- [104] L. Rizzo, A. Fiorentino and A. Anselmo // *Sci. Total Environ.* **427–428** (2012) 263.
- [105] V.M. Sousa, C.M. Manaia, A. Mendes and O.C. Nunes // *J. Photochem. Photobio. A* **251** (2013) 148.
- [106] T.M. Tsai, H.H. Chang, K.C. Chang, Y.L. Liu and C.C. Tseng // *J. Chem. Technol. Biotechnol.* **85** (2010) 1642.
- [107] C. Coulon, A. Collignon, G. McDonnell and V. Thomas // *J. Clin. Microbiol.* **48** (2010) 2689.
- [108] W.L. Nicholson, N. Munakata, G. Horneck, H.J. Melosh and P. Setlow // *Microbiol. Mol. Biol. R.* **64** (2000) 548.
- [109] D. Gummy, A.G. Rincon, R. Hajdu and C. Pulgarin // *Solar Energy* **80** (2006) 1376.
- [110] J.S. Wist, J. Dierolf, C. Torres and W. Pulgarin // *J. Photochem. Photobio. A* (2002) 241.
- [111] J.C. Yu, W. Ho, J. Yu, H. Yip, P.K. Wong and J. Zhao // *Environ. Sci. Technol.* **39** (2005) 1175.
- [112] M. Cho, H. Chung, W. Choi and J. Yoon // *Appl. Environ. Microb.* **71** (2005) 270.
- [113] D.M. Blake, P.C. Maness, Z. Huang, E.J. Wolfrum, J. Huang and W.A. Jacoby // *Sep. Purif. Methods* **28** (1999) 1.
- [114] C. Hu, Y. Lan, J. Qu, X. Hu and A. Wang // *J. Phys. Chem. B* **110** (2006) 4066.
- [115] C. McCullagh, J.M.C. Robertson, D.W. Bahnemann and P.K.J. Robertson // *Res. Chem. Intermed.* **33** (2007) 359.
- [116] J.A. Ibanez, M.I. Litter and R.A. Pizarro // *J. Photochem. Photobio. A* **157** (2003) 81.
- [117] P.S.M. Dunlop, J.A. Byrne, N. Manga and B.R. Eggins // *J. Photochem. Photobio. A* **148** (2002) 355.
- [118] R. Dillert, U. Siemon and D. Bahnemann // *Chem. Eng. Technol.* **21** (1998) 356.
- [119] C.M.B. Carvalho, J.P.C. Tomé, M.A.F. Faustino, M.G.P.M.S. Neves, A.C. Tomé, J.A.S. Cavaleiro, L. Costa, E. Alves, A. Oliveira, Â. Cunha and A. Almeida // *J. Porphyrins Phthalocyanines* **13** (2009) 574.
- [120] J.M.C. Robertson, P.K.J. Robertson and L.A. Lawton // *J. Photochem. Photobio. A* **175** (2005) 51.
- [121] A.G. Rincon and C. Pulgarin // *Catal. Today* **101** (2005) 331.
- [122] M. Wainwright // *Photochem. Photobio. Sci.* **3** (2004) 406.
- [123] M.J. Casteel, K. Jayaraj, A. Gold, L.M. Ball and M.D. Sobsey // *Photochem. Photobiol.* **80** (2004) 294.
- [124] J. Gamage and Z.S. Zhang // *Int. J. Photoenergy* (2010) Article ID 764870.
- [125] Y. Oka, W.C. Kim, T. Yoshida, T. Hirashima, H. Mouri, H. Urade, Y. Itoh and T. Kubo // *J. Biomed. Mater. Res. B* **86B** (2008) 530.
- [126] R. Baan, K. Straif, Y. Grosse, B. Secretan, F. El Ghissassi and V. Coglianò // *Lancet Oncol.* **7** (2006) 295.
- [127] V.L. Colvin // *Nat. Biotech.* **21** (2003) 1166.
- [128] L. Caballero, K.A. Whitehead, N.S. Allen and J. Verran // *J. Photochem. Photobio. A* **276** (2013) 50.
- [129] T. Zuccheri, M. Colonna, I. Stefanini, C. Santini and D. Gioia // *Materials* **6** (2013) 3270.
- [130] K.S. Yao, D.Y. Wang, C.Y. Chang, K.W. Weng, L.Y. Yang, S.J. Lee, T.C. Cheng and C.C. Hwang // *Surf. Coat. Technol.* **202** (2007) 1329.
- [131] E.J. Wolfrum, J. Huang, D.M. Blake, P.-C. Maness, Z. Huang, J. Fiest and W.A. Jacoby // *Environ. Sci. Technol.* **36** (2002) 3412.
- [132] A. Vohra, D.Y. Goswami, D.A. Deshpande and S.S. Block // *J. Ind. Microbiol. Biot.* **32** (2005) 364.
- [133] E.V. Skorb, L.I. Antonouskaya, N.A. Belyasova, D.G. Shchukin, H. Möhwald and D.V. Sviridov // *Appl. Catal. B-Environ* **84** (2008) 94.
- [134] S. Navalon, M. Alvaro, H. Garcia, D. Escrig and V. Costa // *Water Sci. Technol.* **59** (2009) 639.
- [135] J. Lonnen, S. Kilvington, S.C. Kehoe, F. Al-Touati and K.G. McGuigan // *Water Res.* **39** (2005) 877.
- [136] C.-Y. Lin and C.-S. Li // *Aerosol Sci. Technol.* **37** (2003) 162.

- [137] K.P. Kühn, I.F. Chaberny, K. Massholder, M. Stickler, V.W. Benz, H.-G. Sonntag and L. Erdinger // *Chemosphere* **53** (2003) 71.
- [138] S.-C. Kim and D.-K. Lee // *Microchem. J.* **80** (2005) 227.
- [139] M.B. Fisher, D.A. Keane, P. Fernandez-Ibanez, J. Colreavy, S.J. Hinder, K.G. McGuigan and S.C. Pillai // *Appl. Catal. B-Environ.* **130** (2013) 8.
- [140] A. Erkan, U. Bakir and G. Karakas // *J. Photoch. Photobio. A* **184** (2006) 313.
- [141] P.S.M. Dunlop, C.P. Sheeran, J.A. Byrne, M.A.S. McMahon, M.A. Boyle and K.G. McGuigan // *J. Photoch. Photobio. A* **216** (2010) 303.
- [142] C. Chawengkijwanich and Y. Hayata // *Int. J. Food Microbiol.* **123** (2008) 288.
- [143] J.A. Herrera Melián, J.M. Doña Rodríguez, A. Vera Suárez, E. Tello Rendón, C. Valdés do Campo, J. Arana and J. Pérez Peña // *Chemosphere* **41** (2000) 323.
- [144] J. Ângelo, L. Andrade and A. Mendes // *Appl. Catal. A-Gen.* **484** (2014) 17.
- [145] M. Dizdaroglu, P. Jaruga, M. Birincioglu and H. Rodriguez // *Free Radical Biol. Med.* **32** (2002) 1102.
- [146] T. Matsunaga, R. Tomoda, T. Nakajima, N. Nakamura and T. Komine // *Appl. Environ. Microb.* **54** (1988) 1330.
- [147] C. Srinivasan and N. Somasundaram // *Curr. Sci. India* **85** (2003) 8.
- [148] Z. Huang, P.-C. Maness, D.M. Blake, E.J. Wolfrum, S.L. Smolinski and W.A. Jacoby // *J. Photoch. Photobio. A* **130** (2000) 163.
- [149] K. Sunada, T. Watanabe and K. Hashimoto // *J. Photoch. Photobio. A* **156** (2003) 227.
- [150] W. Kangwansupamonkon, V. Lauruengtana, S. Surassmo and U. Ruktanonchai // *Nanomed-Nanotechnol.* **5** (2009) 240.
- [151] L. Luo, L. Miao, S. Tanemura and M. Tanemura // *Mat. Sci. Eng. B* **148** (2008) 183.
- [152] R. van Grieken, J. Marugán, C. Pablos, L. Furones and A. López // *Appl. Catal. B-Environ* **100** (2010) 212.
- [153] Z.X. Lu, L. Zhou, Z.L. Zhang, W.L. Shi, Z.X. Xie, H.Y. Xie, D.W. Pang and P. Shen // *Langmuir* **19** (2003) 8765.
- [154] P. Demchick and A.L. Koch // *J. Bacteriol.* **178** (1996) 768.
- [155] ISO 27447:2009 *Fine ceramics (advanced ceramics, advanced technical ceramics) — Test method for antibacterial activity of semiconducting photocatalytic materials* (ISO, 2009).
- [156] P. Fernández, J. Blanco, C. Sichel and S. Malato // *Catal. Today* **101** (2005) 345.
- [157] A.G. Rincón and C. Pulgarin // *Appl. Catal. B-Environ.* **44** (2003) 263.
- [158] A.K. Benabbou, Z. Derriche, C. Felix, P. Lejeune and C. Guillard // *Appl. Catal. B-Environ.* **76** (2007) 257.
- [159] A. Pal, S.O. Pehkonen, L.E. Yu and M.B. Ray // *Ind. Eng. Chem. Res.* **47** (2008) 7580.
- [160] W.-C.G. Armon and P. Bettane // *Waterborne Pathog.* **4** (2004) 8.
- [161] E.S. Tuchina and V.V. Tuchin // *Laser Phys. Lett.* **7** (2010) 607.
- [162] Y.W. Cheng, R.C.Y. Chan and P.K. Wong // *Water Res.* **41** (2007) 842.
- [163] S. Tanaka, K. Ikeda, H. Miyasaka, Y. Shioi, Y. Suzuki, M. Tamoi, T. Takeda, S. Shigeoka, K. Harada and K. Hirata // *J. Biosci. Bioeng.* **112** (2011) 462.
- [164] S.B. Farr and T. Kogoma // *Microbiol. Rev.* **55** (1991) 561.
- [165] Y.-H. Tsuang, J.-S. Sun, Y.-C. Huang, C.-H. Lu, W.H.-S. Chang and C.-C. Wang // *Artif. Organs* **32** (2008) 167.
- [166] N.S. Allen, M. Edge, G. Sandoval, J. Verran, J. Stratton and J. Maltby // *Photochem. Photobiol.* **81** (2005) 279.
- [167] J. Podporska-Carroll, E. Panaitescu, B. Quilty, L. Wang, L. Menon and S.C. Pillai // *Appl. Catal. B-Environ.* **176–177** (2015) 70.
- [168] U. Joost, K. Juganson, M. Visnapuu, M. Mortimer, A. Kahru, E. Nõmmiste, U. Joost, V. Kisand and A. Ivask // *J. Photoch. Photobio. B* **142** (2015) 178.
- [169] A.C. Miranda, M. Lepretti, L. Rizzo, I. Caputo, V. Vaiano, O. Sacco, W.S. Lopes and D. Sannino // *Sci. Total Environ.* **554–555** (2016) 1.
- [170] B. Kim, D. Kim, D. Cho and S. Cho // *Chemosphere* **52** (2003) 277.
- [171] D. Venieri, E. Markogiannaki, E. Chatzisyneon, E. Diamadopoulos and D. Mantzavinos // *Photoch. Photobio. Sci.* **12** (2013) 645.
- [172] C. Berberidou, I. Paspaltsis, E. Pavlidou, T. Sklaviadis and I. Poullos // *Appl. Catal. B-Environ.* **125** (2012) 375.
- [173] J.-Y. Choi, K.-H. Kim, K.-C. Choy, K.-T. Oh and K.-N. Kim // *J. Biomed. Mater. Res. B* **80B** (2007) 353.

- [174] T. Saito, T. Iwase, J. Horie and T. Morioka // *J. Photoch. Photobio. B* **14** (1992) 369.
- [175] C. Sichel, M. de Cara, J. Tello, J. Blanco and P. Fernández-Ibáñez // *Appl. Catal. B-Environ.* **74** (2007) 152.
- [176] J.H. Lee, M. Kang, S.-J. Choung, K. Ogino, S. Miyata, M.-S. Kim, J.-Y. Park and J.-B. Kim // *Water Res.* **38** (2004) 713.
- [177] M. Agulló-Barceló, M.I. Polo-López, F. Lucena, J. Jofre and P. Fernández-Ibáñez // *Appl. Catal. B-Environ.* **136–137** (2013) 341.
- [178] R.J. Watts, S. Kong, M.P. Orr, G.C. Miller and B.E. Henry // *Water Res.* **29** (1995) 95.
- [179] J. Araña, J.A. Herrera Melián, J.M. Doña Rodríguez, O. González, Pérez Peña, P.M. Marrero Sosa and V. Espino Jiménez // *Catal. Today* **76** (2002) 279.
- [180] C.-H. Lin, R.-F. Yu, W.-P. Cheng and C.-R. Liu // *J. Hazard. Mater.* **209–210** (2012) 348.
- [181] A. Kubacka, M. Ferrer, A. Martínez-Arias and M. Fernández-García // *Appl. Catal. B-Environ.* **84** (2008) 87.
- [182] W.-J. Chen, P.-J. Tsai and Y.-C. Chen // *Small* **4** (2008) 485.
- [183] V. Rodríguez-González, S.O. Alfaro, L.M. Torres-Martínez, S.-H. Cho and S.-W. Lee // *Appl. Catal. B-Environ.* **98** (2010) 229.
- [184] L. Zhang, M.D. Han, O.K. Tan, M.S. Tse, Y.X. Wang and C.C. Sze // *J. Mater. Chem. B* **1** (2013) 564.
- [185] C.-L. Cheng, D.-S. Sun, W.-C. Chu, Y.-H. Tseng, H.-C. Ho, J.-B. Wang, P.-H. Chung, J.-H. Chen, P.-J. Tsai, N.-T. Lin, M.-S. Yu and H.-H. Chang // *J. Biomed. Sci.* **16** (2009) 7.
- [186] O. Akhavan and E. Ghaderi // *J. Phys. Chem. C* **113** (2009) 20214.
- [187] A. Pal, S.O. Pehkonen, L.E. Yu and M.B. Ray // *J. Photoch. Photobio. A* **186** (2007) 335.
- [188] G. Veréb, L. Manczinger, A. Oszkó, A. Sienkiewicz, L. Forró, K. Mogyorósi, A. Dombi and K. Hernádi // *Appl. Catal. B-Environ* **129** (2013) 194.
- [189] O. Akhavan, R. Azimirad, S. Safa and M.M. Larijani // *J. Mater. Chem.* **20** (2010) 7386.
- [190] Y. Lan, C. Hu, X. Hu and J. Qu // *Appl. Catal. B-Environ.* **73** (2007) 354.
- [191] D. Venieri, A. Fraggadaki, M. Kostadima, E. Chatzisyneon, V. Binas, A. Zachopoulos, G. Kiriakidis and D. Mantzavinos // *Appl. Catal. B-Environ* **154–155** (2014) 93.
- [192] K. Pathakoti, S. Morrow, C. Han, M. Pelaez, X. He, D.D. Dionysiou and H.-M. Hwang // *Environ. Sci. Technol.* **47** (2013) 9988.
- [193] R. Sadowski, M. Strus, M. Buchalska, P.B. Heczko and W. Macyk // *Photoch. Photobio. Sci.* **14** (2015) 514.
- [194] P. Gao, A. Li, D.D. Sun and W.J. Ng // *J. Hazard. Mater.* **279** (2014) 96.
- [195] H.M. Yadav, T.V. Kolekar, S.H. Pawar and J.-S. Kim // *J. Mater. Sci-Mater. M.* **27** (2016) 1.
- [196] P. Magalhães, J. Ângelo, V.M. Sousa, O.C. Nunes, L. Andrade and A. Mendes // *Biochem. Eng. J.* **104** (2015) 20.
- [197] D.-H. Kuo, W.-T. Hsu and Y.-Y. Yang // *Appl. Catal. B-Environ* **184** (2016) 191.
- [198] Y.-H. Tseng, D.-S. Sun, W.-S. Wu, H. Chan, M.-S. Syue, H.-C. Ho and H.-H. Chang // *BBA - Gen. Subjects* (2013).
- [199] W.A. Rutala and D.J. Weber // *Clin. Microbiol. Rev.* **10** (1997) 597.
- [200] M. Deborde and U. von Gunten // *Water Res.* **42** (2008) 13.
- [201] A.V. Levanov, I.V. Kuskov, E.E. Antipenko and V.V. Lunin // *Russ. J. Phys. Chem.* **86** (2012) 757.
- [202] J.C. Crittenden, M.W. Harza, D.W. Hand and K.J. Howe, *MWH's Water Treatment: Principles and Design* (Wiley, 2012).
- [203] W.A. Rutala and D.J. Weber, *C.f.D. Control, Guideline for disinfection and sterilization in healthcare facilities* (Centers for Disease Control, 2008).
- [204] V. Lazarova, P. Savoye, M.L. Janex, E.R. Blatchley Iii and M. Pommepuy // *Water Sci. Technol.* **40** (1999) 203.
- [205] G.P. Winward, L.M. Avery, T. Stephenson and B. Jefferson // *Water Res.* **42** (2008) 483.
- [206] R. Virto, P. Mañas, I. Álvarez, S. Condon and J. Raso // *Appl. Environ. Microb.* **71** (2005) 5022.
- [207] C. Shang and E.R. Blatchley Iii // *Water Res.* **35** (2001) 244.
- [208] A. Hassen, A. Heyouni, H. Shayeb, M. Cherif and A. Boudabous // *Bioresour. Technol.* **72** (2000) 85.
- [209] L.V. Venczel, M. Arrowood, M. Hurd and M.D. Sobsey // *Appl. Environ. Microb.* **63** (1997) 1598.
- [210] G. Berg, D.R. Dahling, G.A. Brown and D. Berman // *Appl. Environ. Microb.* **36** (1978) 880.

- [211] J.A. Tree, M.R. Adams and D.N. Lees // *Appl. Environ. Microb.* **69** (2003) 2038.
- [212] J. Koivunen and H. Heinonen-Tanski // *Water Res.* **39** (2005) 1519.
- [213] C.H. King, E.B. Shotts, R.E. Wooley and K.G. Porter // *Appl. Environ. Microb.* **54** (1988) 3023.
- [214] S. Neralla, R.W. Weaver, B.J. Lesikar and R.A. Persyn // *Bioresour. Technol.* **75** (2000) 19.
- [215] T.E. Agustina, H.M. Ang and V.K. Vareek // *Appl. Environ. Microb.* **6** (2005) 264.
- [216] J. Hoigné and H. Bader // *Water Res.* **17** (1983) 173.
- [217] J.A. Imlay // *Nat. Rev. Micro.* **11** (2013) 443.
- [218] C.-S. Li and Y.-C. Wang // *AIHA Journal* **64** (2003) 533.
- [219] H. Liltved, H. Hektoen and H. Efraimsen // *Aquacult. Eng.* **14** (1995) 107.
- [220] C. Nebel, R.D. Gottschling, R.L. Hutchison, T.J. McBride, D.M. Taylor, J.L. Pavoni, M.E. Tittlebaum, H.E. Spencer and M. Fleischman // *J. Water Pollut. Control. Fed.* **45** (1973) 2493.
- [221] J.C. Joret, J.C. Block and Y. Richard // *Ozone-Sci. Eng.* **4** (1982) 91.
- [222] M.L. Janex, P. Savoye, M. Roustan, Z. Do-Quang, J.M. Laîné and V. Lazarova // *Ozone-Sci. Eng.* **22** (2000) 113.
- [223] J.M. Sousa, G. Macedo, M. Pedrosa, C. Becerra-Castro, S. Castro-Silva, M.F.R. Pereira, A.M.T. Silva, O.C. Nunes and C.M. Manaia // *J. Hazard. Mater.* **323A** (2017) 434.
- [224] J.G. Kim and A.E. Yousef // *J. Food Sci.* **65** (2000) 521.
- [225] G.R. Burlison, T.M. Murray and M. Pollard // *Appl. Microbiol.* **29** (1975) 340.
- [226] G.H.R. Silva, L.A. Daniel, H. Bruning and W.H. Rulkens // *Bioresour. Technol.* **101** (2010) 6981.
- [227] J.L. Rennecker, B.J. Mariñas, J.H. Owens and E.W. Rice // *Water Res.* **33** (1999) 2481.
- [228] S.K. Sastry, A.K. Datta and R.W. Worobo // *J. Food Sci.* **65** (2000) 90.
- [229] WHO (World Health Organization) *Guidelines for Drinking-water Quality* (WHO, Geneva, Switzerland, 2011).
- [230] C. Bouki, D. Venieri and E. Diamadopoulos // *Ecotox. Environ. Safe.* **91** (2013) 1.
- [231] M.-T. Guo, Q.-B. Yuan and J. Yang // *Water Res.* **47** (2013) 6388.
- [232] N. Goosen and G.F. Moolenaar // *DNA Repair* **7** (2008) 353.
- [233] R.P. Rastogi, Richa, A. Kumar, M.B. Tyagi and R.P. Sinha // *J. Nucleic Acids* **2010** (2010).
- [234] R.P. Sinha and D.-P. Hader // *Photoch. Photobio. Sci.* **1** (2002) 225.
- [235] A.L. Santos, C. Moreirinha, D. Lopes, A.C. Esteves, I. Henriques, A. Almeida, M.R.M. Domingues, I. Delgadillo, A. Correia and Â. Cunha // *Environ. Sci. Technol.* **47** (2013) 6306.
- [236] K.G. McGuigan, R.M. Conroy, H.-J. Mosler, M.d. Preez, E. Ubomba-Jaswa and P. Fernandez-Ibañez // *J. Hazard. Mater.* **235–236** (2012) 29.
- [237] L. Rizzo, C. Manaia, C. Merlin, T. Schwartz, C. Dagot, M.C. Ploy, I. Michael and D. Fatta-Kassinos // *Sci. Total Environ.* **447** (2013) 345.
- [238] W.A.M. Hijnen, E.F. Beerendonk and G.J. Medema // *Water Res.* **40** (2006) 3.
- [239] T. Bintsis, E. Litopoulou-Tzanetaki and R.K. Robinson // *J. Sci. Food Agric.* **80** (2000) 637.
- [240] E. Levetin, R. Shaughnessy, C.A. Rogers, R. Scheir // *Appl. Environ. Microb.*, **67** (2001) 3712-3715.
- [241] W.A. Rutala, M.F. Gergen and D.J. Weber // *Infect. Cont. Hosp. Ep.* **31** (2010) 1025.
- [242] C.W. McKinney and A. Pruden // *Environ. Sci. Technol.* **46** (2012) 13393.
- [243] J.C. Chang, S.F. Ossoff, D.C. Lobe, M.H. Dorfman, C.M. Dumais, R.G. Qualls and J.D. Johnson // *Appl. Environ. Microb.* **49** (1985) 1361.
- [244] P. Drogui, S. Elmaleh, M. Rumeau, C. Bernard and A. Rambaud // *J. Appl. Electrochem.* **31** (2001) 877.
- [245] F. Haber and J. Weiss, *The Catalytic Decomposition of Hydrogen Peroxide by Iron Salts* (1934).
- [246] J.P. Kehrer // *Toxicology* **149** (2000) 43.
- [247] E. Linley, S.P. Denyer, G. McDonnell, C. Simons and J.-Y. Maillard // *J. Antimicrob. Chemother.* **67** (2012) 1589.
- [248] M. Finnegan, E. Linley, S.P. Denyer, G. McDonnell, C. Simons and J.-Y. Maillard // *J. Antimicrob. Chemother.* **65** (2010) 2108.
- [249] G. Fichet, E. Comoy, C. Duval, K. Antloga, C. Dehen, A. Charbonnier, G. McDonnell, P. Brown, C. Ida Lasmézas and J.-P. Deslys // *The Lancet* **364** (2004) 521.

- [250] G. Fichet, K. Antloga, E. Comoy, J.P. Deslys and G. McDonnell // *J. Hosp. Infect.* **67** (2007) 278.
- [251] J.A. Otter and G.L. French // *J. Clin. Microbiol.* **47** (2009) 205.
- [252] N.A. Klapes and D. Vesley // *Appl. Environ. Microb.* **56** (1990) 503.
- [253] M. Ksibi // *Chem. Eng. J.* **119** (2006) 161.
- [254] S. Lemmen, S. Scheithauer, H. Häfner, S. Yezli, M. Mohr and J.A. Otter // *Am. J. Infect. Control* **43** (2015) 82.
- [255] *Water treatment manual: disinfection* (United States Environmental Protection Agency, 2011).
- [256] J. Gamage and Z. Zhang // *Int. J. Photoenergy* **2010** (2010).
- [257] D. Spasiano, R. Marotta, S. Malato, P. Fernandez-Ibañez and I. Di Somma // *Appl. Catal. B-Environ* **170–171** (2015) 90.
- [258] M.S. Siddiqui, G.L. Amy and R.G. Rice // *J. Am. Water Works Ass.* **87** (1995) 58.
- [259] L. Rizzo, H. Selcuk, A.D. Nikolaou, S. Meriç Pagano and V. Belgiorno // *Desalin. Water Treat.* **52** (2013) 1414.
- [260] L. Prieto-Rodríguez, I. Oller, N. Klammerth, A. Agüera, E.M. Rodríguez and S. Malato // *Water Res.* **47** (2013) 1521.
- [261] N.F.F. Moreira, J.M. Sousa, G. Macedo, A.R. Ribeiro, L. Barreiros, M. Pedrosa, J.L. Faria, M.F.R. Pereira, S. Castro-Silva, M.A. Segundo, C.M. Manaia, O.C. Nunes and A.M.T. Silva // *Water Res.* **94** (2016) 10.
- [262] C. Blazejewski, F. Wallet, A. Rouzé, R. Le Guern, S. Ponthieux, J. Salleron and S. Nseir // *Critical Care* **19** (2015) 30.
- [263] K.E. Wainwright, M. Lagunas-Solar, M.A. Miller, B.C. Barr, I.A. Gardner, C. Pina, A.C. Melli, A.E. Packham, N. Zeng, T. Truong and P.A. Conrad // *Appl. Environ. Microb.* **73** (2007) 5663.
- [264] M.W. LeChevallier, C.D. Cawthon and R.G. Lee // *Appl. Environ. Microb.* **54** (1988) 649.
- [265] O.K. Dalrymple, E. Stefanakos, M.A. Trotz and D.Y. Goswami // *Appl. Catal. B-Environ* **98** (2010) 27.
- [266] G.A. Boorman // *Environ. Health Perspect.* **107** (1999) 207.
- [267] P.S.M. Dunlop, M. Ciavola, L. Rizzo, D.A. McDowell and J.A. Byrne // *Catal. Today* **240 Part A** (2015) 55.
- [268] D. Nozaic // *Water Sa* **30** (2004) 18.
- [269] R.G. Rice // *Ozone-Sci. Eng.* **21** (1999) 99.
- [270] V. Camel and A. Bermond // *Water Res.* **32** (1998) 3208.
- [271] *Wastewater technology fact sheet [electronic resource]: ozone disinfection* (United States Environmental Protection Agency, Office of Water, Washington, D.C., 1999).
- [272] *Wastewater technology fact sheet [electronic resource] : ultraviolet disinfection* (United States Environmental Protection Agency, Office of Water, Washington, D.C., 1999).
- [273] G. McDonnell and A.D. Russell // *Clin. Microbiol. Rev.* **12** (1999) 147.
- [274] S. Malato, P. Fernández-Ibañez, M.I. Maldonado, J. Blanco and W. Gernjak // *Catal. Today* **147** (2009) 1.
- [275] Q. Li, S. Mahendra, D.Y. Lyon, L. Brunet, M.V. Liga, D. Li and P.J.J. Alvarez // *Water Res.* **42** (2008) 4591.